


Optimum capacity and full counting statistics of information content and heat quantity in the steady state

Yasuhiro Utsumi

Department of Physics Engineering, Faculty of Engineering, Mie University, Tsu, Mie 514-8507, Japan

 (Received 9 July 2018; revised manuscript received 11 February 2019; published 13 March 2019)

We consider a bipartite quantum conductor and analyze fluctuations of heat quantity in a subsystem as well as self-information associated with the reduced-density matrix of the subsystem. By exploiting the multicontour Keldysh technique, we calculate the Rényi entropy, or the information-generating function, subjected to the constraint of the *local* heat quantity of the subsystem, from which the probability distribution of conditional self-information is derived. We present an equality that relates the optimum capacity of information transmission and the Rényi entropy of order 0, which is the number of integer partitions into distinct parts. We apply our formalism to a two-terminal quantum dot. We point out that in the steady state, the reduced-density matrix and the operator of the *local* heat quantity of the subsystem may be commutative.

DOI: [10.1103/PhysRevB.99.115310](https://doi.org/10.1103/PhysRevB.99.115310)

I. INTRODUCTION

The laws of physics limit the performance of information processing [1–4]. The quantum limits of information transmission through a quantum communication channel have long been discussed [1,4–10]. In information theory, a model communication system consists of a transmitter, a channel, and a receiver [11] [Fig. 1(a)]. The physically relevant part is the channel through which a signal produced by the transmitter reaches the receiver. A measure of the performance of a channel is capacity C , the maximum possible rate at which information can be transmitted without error. More precisely, let I be the amount of information content transmitted during a given measurement time τ . Then, the rate of information transmission always satisfies $I/\tau \leq C$. The capacity of a wide-band quantum channel for a given average signal power P is [5,6,8–10] (we set $\hbar = k_B = e = 1$)

$$C_{\text{WB}}(P) = \sqrt{\frac{\pi}{3} N_{\text{ch}} P}, \quad (1)$$

where N_{ch} is the number of channels. For a fermionic channel [8,10], when the information is carried by electrons, $N_{\text{ch}} = \frac{1}{2}$. For a bosonic channel [5,7,9,10] and for a fermionic channel with electrons and holes, $N_{\text{ch}} = 1$.

The square-root dependence on P of Eq. (1) can be deduced from the energy-time uncertainty relation [1,4,8]. Here, we briefly estimate the capacity following Ref. [8]. Roughly speaking, it is not possible to distinguish energy quanta smaller than $\delta E \sim \hbar/(2\tau)$ [1,8] (see also Ref. [4]). Suppose one bit of information content is conveyed by the arrival or nonarrival of an electron. Since there are N_{ch} channels, an energy window larger than $I\delta E/N_{\text{ch}}$ is needed in order to send I bits of information content. This energy window is accompanied by the energy current, i.e., the signal power, which is estimated by using the Landauer formula for heat current [12] as $P = E/\tau \geq N_{\text{ch}} \hbar^{-1} \int_0^{I\delta E/N_{\text{ch}}} E' dE' = (I\delta E)^2/(2\hbar N_{\text{ch}})$. By rewriting this inequality as $I \leq \sqrt{2\hbar N_{\text{ch}} P}/\delta E$, and by

replacing δE with $\hbar/(2\tau)$, we obtain $I/\tau \leq 4\sqrt{\pi N_{\text{ch}} P}$, which is consistent with Eq. (1).

In information theory, the channel capacity is defined as the mutual information per second between input signal and output signal maximized with respect to the distribution of the input signal [11]. Equation (1) is indeed the *optimum capacity* C_{opt} , which is the capacity further maximized with respect to input states and output measurement schemes [9]. The optimum capacity is the logarithm of the size of the Fock subspace containing electrons with total energy $E = P\tau$. It turned out that the optimum capacity is the *partition function* of the theory of partition [13], i.e., the number of ways to write a positive integer as the sum of positive integers that satisfy a certain condition depending on the statistics of particles [9,10].

In this paper, we discuss information transmission through a mesoscopic quantum electric conductor connected to a left lead and a right lead. We regard the right lead as the transmitter generating thermal and shot noise as signals and regard the quantum conductor as the channel. The left lead corresponds to the receiver side [see Fig. 1(b)]. Temperatures and chemical potentials of the receiver side and the transmitter side can be different. We will set the energy origin at the chemical potential. Therefore, the signal power P would be the heat current Q/τ rather than the energy current E/τ .

In the previous theories [5,6,8–10], an ideal quantum channel was considered. For mesoscopic quantum electric conductors, the scattering theory was developed to analyze the entropy current [12] as well as the capacity [14]. However, there are not many works in this direction. In this paper, we analyze the information content obtained by the receiver side. For this purpose, we bipartition the whole system into the receiver side (subsystem A) and the transmitter side (subsystem B), which includes the channel [Fig. 1(b)]. Subsystem A consists of the left lead. Subsystem B consists of the right lead and the quantum conductor. We introduce a reduced-density matrix of subsystem A by tracing out subsystem B degrees of freedom,

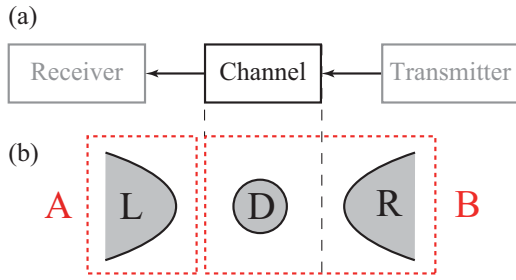


FIG. 1. (a) A model of the communication system. A transmitter-generated signal is sent through a channel to a receiver. We focus on the signal transmission process through the channel. (b) A quantum conductor (single-level quantum dot) coupled to the left and right leads. We regard the quantum conductor as the communication channel. The right lead corresponds to the transmitter, which generates thermal and shot noise as signals. The left lead corresponds to the receiver side. The electron temperature of the left lead is set to zero in order to suppress the intrinsic thermal noise in the receiver side. We regard the left lead as subsystem A and the quantum conductor and the right lead as subsystem B .

$\hat{\rho}_A = \text{Tr}_B \hat{\rho}$. Then, we perform a projective measurement of “local heat quantity” of subsystem A , Q_A , or its dimensionless equivalent $S_A = \beta_A Q_A$, where β_A is the inverse temperature of subsystem A . The reduced-density matrix after obtaining outcome S_A is

$$\hat{\rho}_{A,S_A} = \frac{\hat{\Pi}_{S_A} \hat{\rho}_A \hat{\Pi}_{S_A}}{P(S_A)}, \quad P(S_A) = \text{Tr}_A(\hat{\Pi}_{S_A} \hat{\rho}_A), \quad (2)$$

where $\hat{\Pi}_{S_A}$ is a projection operator and $P(S_A)$ is the probability of obtaining the measurement outcome S_A . The operator of the conditional self-information [15] associated with the state of electrons with signal power $P_A = Q_A/\tau$ would be $\hat{J} = -\ln \hat{\rho}_{A,S_A}$ (hereafter, we choose base e). The operator \hat{J} is formally the “entanglement Hamiltonian” [16–18] subjected to the “local heat quantity” constraint. The purpose of this paper is to analyze the probability distribution of the conditional self-information beyond its average value, i.e., the conditional entropy. In fact, the conditional self-information is a random variable, and thus one can consider its probability distribution function

$$P_{S_A}(J) = \text{Tr}_A[\hat{\rho}_{A,S_A} \delta(J + \ln \hat{\rho}_{A,S_A})]. \quad (3)$$

By exploiting the orthonormal decomposition of the density matrix $\hat{\rho}_{A,S_A} = \sum_n p_n |n\rangle \langle n|$, where $|n\rangle$ is an orthonormal set and p_n are eigenvalues of $\hat{\rho}_{A,S_A}$, the probability distribution function is written as $P_{S_A}(J) = \sum_n p_n \delta(J + \ln p_n)$ (see, e.g., Chap. 2.7 in Ref. [19]). It is convenient to introduce the characteristic function or the information-generating function [20,21], the Fourier transform of the probability distribution function $\int dJ e^{i\xi J} P_{S_A}(J) = \sum_n p_n^{1-i\xi}$, which may be regarded as the Rényi entropy of order $\alpha = 1 - i\xi$ [22,23]. As we will see later in Eq. (19), the Fourier transform of the probability distribution function (3) is related to the Rényi entropy of order M :

$$S_M(S_A) = \text{Tr}_A[(\hat{\Pi}_{S_A} \hat{\rho}_A \hat{\Pi}_{S_A})^M]. \quad (4)$$

The main message of this paper is that, when the thermal noise of the receiver side is suppressed $\beta_A \rightarrow \infty$, there exists a

universal relation similar to Jarzynski equality [24,25], which connects the probability distribution of the conditional self-information, the Rényi entropy of order 0, and the optimum capacity

$$\langle e^J \rangle_{Q_A} = S_0(Q_A) \approx \exp[\tau C_{\text{opt}}(P_A)]. \quad (5)$$

We demonstrate that in our case, Eq. (5) is the partition function of integer partitions into distinct parts.

Here, we note a subtle issue concerning the definition of the operator of the “local heat quantity” of subsystem A . In general, the reduced-density matrix is not diagonal in the eigenbasis of the operator of “local heat quantity” [$\hat{\rho}_A, \hat{Q}_A \neq 0$ [see Eq. (9) for the definition of \hat{Q}_A]]. It is a manifestation of the noncommutativity between the Hamiltonian of the subsystem A , \hat{H}_A , and the full Hamiltonian

$$\hat{H} = \hat{H}_A + \hat{H}_B + \hat{V}, \quad (6)$$

which includes the coupling between the two subsystems \hat{V} . This noncommutativity causes difficulties in constructing the thermodynamics of an open quantum system coupled strongly to reservoirs [26–30]. In our case, it causes difficulties in dealing with the projection operator in Eq. (4). In this paper, we concentrate on the steady state, where the time translational invariance is restored and the coupling energy is neglected as compared with the net energy transfer between the subsystems. In such a case, we can regard [$\hat{\rho}_A, \hat{Q}_A \approx 0$] and circumvent this problem.

Another purpose of this paper is to extend the multicontour Keldysh Green function technique [31–36]. From this point of view, this paper relies on our previous works [33–35]. In Ref. [33], we developed the replica trick to calculate the Rényi entropy in the nonequilibrium steady state. In Ref. [34], we accounted for the local particle-number constraint to analyze the accessible entanglement. In this paper, we will account for the local heat quantity constraint (35b) and (35c). In this way, we are able to calculate the information channel capacity subjected to signal power constraint, which connects thermodynamics and communication theory. A celebrated paper by Shannon [11] demonstrated that the channel capacity of the Gaussian channel depends on the bandwidth B , the average signal power P , and the noise power P_{noise} as $C = B \ln(1 + P/P_{\text{noise}})$. In this paper, we discuss the quantum version of the channel capacity. The flows of Rényi entropy and energy have been discussed also in Ref. [36].

The structure of the paper is as follows. In Sec. II, we introduce probability distributions and information-generating functions. Then, we present a universal relation (21). In Sec. III, we summarize the multicontour Keldysh generating function [31–36]. In Sec. IV, we apply our formalism to a resonant-level model, and then in Sec. V we derive the optimum capacity. In Sec. VI, we focus on energy-independent transmission cases. In Sec. VII, we turn to the resonant tunneling condition. We also discuss the commutability of the reduced-density matrix and the operator of the “local heat quantity” in the presence of the Coulomb interaction in Sec. VII B. In Sec. VIII, we discuss differences between our approach and the previous quantum information theory approach [9,10]. In Sec. IX, we summarize our findings.

II. INFORMATION-GENERATING FUNCTION

A. Joint probability distribution and conditional probability distribution

We assume that initially the two subsystems A and B are decoupled. Each subsystem is in equilibrium:

$$\hat{\rho}_{A(B)\text{eq}} = e^{-\beta_{A(B)}(\hat{H}_{A(B)} - \mu_{A(B)}\hat{N}_{A(B)})} / Z_{A(B)\text{eq}}, \quad (7)$$

where $\beta_{A(B)}$ and $\mu_{A(B)}$ are the inverse temperature and the chemical potential of subsystem $A(B)$, respectively. The equilibrium partition function $Z_{A(B)\text{eq}}$ ensures the normalization condition $\text{Tr}_{A(B)}\hat{\rho}_{A(B)\text{eq}} = 1$. Explicitly, the initial density matrix is $\hat{\rho}(t < 0) = \hat{\rho}_{A\text{eq}}\hat{\rho}_{B\text{eq}}$. At $t = 0$, we switch on the coupling \hat{V} and let the total system evolve until $t = \tau$. Then, we trace out the subsystem B and obtain the reduced-density matrix of the subsystem A as

$$\hat{\rho}_A(\tau) = \text{Tr}_B\hat{\rho}(\tau), \quad \hat{\rho}(\tau) = e^{-i\hat{H}\tau}\hat{\rho}_{A\text{eq}}\hat{\rho}_{B\text{eq}}e^{i\hat{H}\tau}. \quad (8)$$

A naive definition of the operator of the local heat quantity of the subsystem A would be

$$\hat{Q}_A = \hat{S}_A / \beta_A = -\ln \hat{\rho}_{A\text{eq}} / \beta_A. \quad (9)$$

Precisely, Eq. (9) is the operator of energy measured from the chemical potential minus the equilibrium free energy of the subsystem A . In thermodynamics, the heat is not a state function and is defined associated to a certain process. In our case, the process corresponds to the exchange of heat and electrons between the subsystem A and the exterior, the subsystem B . Indeed, the time derivative of the average of the operator (9) is compatible with the commonly used definition of the heat flux (see Ref. [28] for definitions of the heat)

$$\frac{d}{dt}\langle \hat{Q}_A(t) \rangle = \dot{E}_A(t) - \mu_A \dot{N}_A(t). \quad (10)$$

Here, the averages of energy and particle currents are $\dot{E}_A(t) = -i \text{Tr}(\hat{\rho}(t)[\hat{H}_A, \hat{H}])$ and $\dot{N}_A(t) = -i \text{Tr}(\hat{\rho}(t)[\hat{N}_A, \hat{H}])$, respectively. Once we accept Eq. (9), the projection operator can be written as (Appendix A)

$$\hat{\Pi}_{S_A} = \frac{\Delta}{2\pi} \int_{-\pi/\Delta}^{\pi/\Delta} d\chi e^{-i\chi S_A} \hat{\rho}_{A\text{eq}}^{-i\chi}. \quad (11)$$

For simplicity, we assume that the dimensionless heat quantity is discrete $S_A = \Delta n$, where n is an integer. Δ is a small number, and we set $\Delta \rightarrow +0$ at the end of the calculations. Physically, this operation would correspond to taking the limit of large subsystem size in the end of calculations. As far as $\Delta > 0$, $S_A \in (-\infty, \infty)$ and thus there would be no limitation on the bandwidth of the detector, i.e., the subsystem A .

The reduced-density matrix after the projective measurement is $\hat{\rho}'_A = \sum_{S_A} P(S_A) \hat{\rho}_{A,S_A}$. We define the joint probability distribution function of self-information content and dimensionless heat quantity as

$$P(I'_A, S_A) = \text{Tr}_A[\hat{\Pi}_{S_A} \hat{\rho}_A \hat{\Pi}_{S_A} \delta(I'_A + \ln \hat{\rho}'_A)]. \quad (12)$$

By using the joint probability distribution function, the probability distribution function of conditional self-information (3) can be written as

$$P_{S_A}(J) = P(I'_A = J - \ln P(S_A), S_A) / P(S_A). \quad (13)$$

The information-generating function of the joint probability distribution (12) is

$$\begin{aligned} S_{1-i\xi}(S_A) &= \int dI'_A e^{i\xi I'_A} P(I'_A, S_A) \\ &= \text{Tr}_A[(\hat{\Pi}_{S_A} \hat{\rho}_A \hat{\Pi}_{S_A})^{1-i\xi}]. \end{aligned} \quad (14)$$

We call the parameter of Fourier transform ξ the ‘‘counting field.’’ By performing the analytic continuation $1 - i\xi \rightarrow M$, we obtain the Rényi entropy (4). Because of their apparent similarity, we use the terms ‘‘information-generating function’’ and ‘‘Rényi entropy’’ interchangeably.

We further perform the Fourier transform in terms of the dimensionless heat quantity. By exploiting the expression (11), we obtain

$$S_{1-i\xi}(\chi) = \sum_{S_A} e^{i\chi S_A} S_{1-i\xi}(S_A) = \text{Tr}_A(\hat{\rho}_A'^{1-i\xi} \hat{\rho}_{A\text{eq}}^{-i\chi}). \quad (15)$$

Once the Rényi entropy (15) is obtained, the joint probability distribution is recovered by performing the inverse Fourier transform. In this paper, we focus on the steady state realized in the limit of $\tau \rightarrow \infty$. In the presence of a finite affinity, the temperature difference or the chemical potential difference, the number of exchanged electrons grows linearly in the measurement time τ . Since the information is conveyed by arrivals or nonarrivals of electrons, the self-information content as well as the heat quantity would grow in proportion to the measurement time τ [33,34]. Therefore, the inverse Fourier transform can be done within the saddle-point approximation

$$P(I'_A, S_A) = \frac{1}{2\pi} \int d\xi e^{-i\xi I'_A} S_{1-i\xi}(S_A) \quad (16a)$$

$$\approx \exp\left[\min_{i\xi \in \mathbb{R}} [\ln S_{1-i\xi}(S_A) - i\xi I'_A]\right], \quad (16b)$$

which is the Legendre-Fenchel transform [37]. For the joint probability distribution, we can perform the double Legendre transform

$$\ln P(I'_A, S_A) \approx \min_{i\xi, i\chi \in \mathbb{R}} [\ln S_{1-i\xi}(\chi) - i\xi I'_A - i\chi S_A]. \quad (17)$$

Hereafter, we use S_A and Q_A interchangeably. The two quantities and corresponding counting fields χ and X are related as $Q_A = S_A / \beta_A$ and $X = \beta_A \chi$, respectively. The joint cumulant between self-information and heat quantity is obtained by a derivative of the information-generating function

$$\langle\langle I'_A{}^\ell Q_A^m \rangle\rangle = \partial_{i\xi}^\ell \partial_{i\chi}^m \ln S_{1-i\xi}(\chi) \Big|_{\xi=X=0}. \quad (18)$$

B. Universal relation and optimum capacity

The information-generating function of the probability distribution of conditional self-information (13) is

$$S_{1-i\xi, S_A} = \int dJ e^{i\xi J} P_{S_A}(J) = \frac{S_{1-i\xi}(S_A)}{S_1(S_A)^{1-i\xi}}. \quad (19)$$

The first derivative gives the von Neumann entropy [38] $S(\hat{\rho}) = -\text{Tr}\hat{\rho} \ln \hat{\rho}$ as

$$\langle\langle J \rangle\rangle = \partial_{i\xi} \ln S_{1-i\xi, S_A} \Big|_{i\xi=0} = S(\hat{\rho}_{A, S_A}). \quad (20)$$

The information-generating function satisfies a Jarzynski equality [24,25] like universal relation

$$\begin{aligned} \langle e^J \rangle_{S_A} &= \int dJ e^J P_{S_A}(J) = \int dJ \text{Tr}_A[\delta(J - \hat{J})] \\ &= S_{0,S_A} = \text{rank } \hat{\rho}_{A,S_A} \\ &= S_0(S_A) = \text{rank}(\hat{\Pi}_{S_A} \hat{\rho}_A \hat{\Pi}_{S_A}). \end{aligned} \quad (21)$$

The last expression of the first line means the number of eigenvalues of the ‘‘entanglement Hamiltonian’’ [16–18] $\hat{J} = -\ln \hat{\rho}_{A,S_A}$. The last equation of the second line means the number of *positive* eigenvalues of the reduced-density matrix $\hat{\rho}_{A,S_A}$. Therefore, $\langle e^J \rangle_{S_A}$ would represent the number of all possible many-body electron states in the subsystem A for a given local dimensionless heat quantity S_A occurring with positive probabilities. In general, the zeroth-order Rényi entropy gives the measure of the support set of a given probability density function, while the Shannon entropy gives the size of the effective support set [15].

To proceed, we perform the Fourier transform of Eq. (21), $S_0(X) = \sum_{Q_A} e^{iX Q_A} \langle e^J \rangle_{Q_A} = \text{Tr}_A(\hat{\rho}_A^0 \hat{\rho}_{\text{Aeq}}^{-iX/\beta_A})$, and then perform the inverse Fourier transform within the saddle-point approximation

$$\begin{aligned} \ln \langle e^J \rangle_{Q_A} &= \ln \frac{\Delta}{2\pi\beta_A} \int_{-\pi\beta_A/\Delta}^{\pi\beta_A/\Delta} dX e^{-iX Q_A} S_0(X) \\ &\approx \min_{i\lambda \in \mathbb{R}} [\ln S_0(X = \lambda/\Delta E) - i\lambda n], \end{aligned} \quad (22)$$

where we introduced the heat quantity divided by the energy resolution $\Delta E = h/(2N_{\text{ch}}\tau)$, $n = Q_A/\Delta E = \tau^2 N_{\text{ch}} P_A/\pi$. In Sec. VB, we calculate the second line of Eq. (22) in the limit of $\beta_A \rightarrow \infty$ explicitly for a resonant-level model and reproduce the optimum capacity in the previous works [9,10] Eq. (56) as claimed by Eq. (5).

If $P_{Q_A}(J) \geq 0$, by exploiting Jensen’s inequality and the universal relations (5) and (21), one can check that the average conditional self-information is bounded from above:

$$\langle J \rangle_{Q_A} = S(\hat{\rho}_{A,Q_A}) \leq \ln \text{rank } \hat{\rho}_{A,Q_A} = \tau C_{\text{opt}}(P). \quad (23)$$

Here, we comment on the definition of the delta function in Eqs. (3) and (12) and the normalization condition of the joint probability distribution (12). By using the spectral decomposition of the reduced-density matrix,

$$\hat{\rho}'_A = \sum_j \lambda_j |j\rangle\langle j|, \quad (24)$$

where λ_j are non-negative eigenvalues, the delta function in Eqs. (3) and (12) is defined as

$$\delta(I'_A + \ln \hat{\rho}'_A) = \sum_{j \in \mathcal{S}} |j\rangle\langle j| \delta(I'_A + \ln \lambda_j). \quad (25)$$

Here, the summation is performed over the index j associated with positive eigenvalues $\mathcal{S} = \{j : \lambda_j > 0\}$. In this paper, we will assume that the initial state of the subsystem A is in a pure state:

$$\rho_{\text{Aeq}} = |\text{FS}\rangle\langle \text{FS}|, \quad (26)$$

where $|\text{FS}\rangle$ is a unique ground-state many-body wave function (at the ground state, electrons fill up to the Fermi energy).

Then,

$$\int dI'_A \int dS_A P(I'_A, S_A) = S_1(\chi = 0) = \sum_{j \in \mathcal{S}} |\langle j|\text{FS}\rangle|^2, \quad (27)$$

which would not necessarily be 1. In this paper, we will consider a specific model, a resonance-level model, and check the normalization condition through explicit calculations [see Eq. (52)].

III. MULTICONTOUR KELDYSH TECHNIQUE

A. Bulk contribution

Let us calculate the Rényi entropy (15) at the initial state $\tau = 0$, in which the two subsystems are decoupled:

$$s_M(\chi) = \text{Tr}_B(\hat{\rho}_{\text{Aeq}}^{M-i\chi}), \quad (28)$$

where we used $\hat{\rho}'_A = \hat{\rho}_{\text{Aeq}}$. The operators of the Hamiltonian and particle number of the subsystem A are

$$\hat{H}_A = \sum_k \epsilon_{Ak} \hat{a}_{Ak}^\dagger \hat{a}_{Ak}, \quad (29a)$$

$$\hat{N}_A = \sum_k \hat{a}_{Ak}^\dagger \hat{a}_{Ak}. \quad (29b)$$

Then, the unperturbed part (28) reads as

$$\ln s_M(\chi) = \ln \frac{\text{Tr}_A e^{-(M-i\chi)\beta_A(\hat{H}_A - \mu_A \hat{N}_A)}}{Z_{\text{Aeq}}^{M-i\chi}} \quad (30)$$

$$= \ln \frac{\prod_k (1 + e^{-(M-i\chi)\beta_A(\epsilon_{Ak} - \mu_A)})}{\prod_k (1 + e^{-\beta_A(\epsilon_{Ak} - \mu_A)})^{M-i\chi}} \quad (31)$$

$$= \int d\omega \mathcal{N}_A(\omega) \ln [f_A^+(\omega)^{M-i\chi} + f_A^-(\omega)^{M-i\chi}], \quad (32)$$

where $\mathcal{N}_A(\omega) = \sum_k \delta(\omega - \epsilon_{Ak})$ is the density of states (DOS) of the subsystem A . The electron (hole) distribution function is

$$f_A^\pm(\omega) = \frac{1}{1 + e^{\pm\beta_A(\omega - \mu_A)}}. \quad (33)$$

For further calculations, we assume the DOS is energy independent $\mathcal{N}_A(\omega) = V_A \rho_A$, where V_A is the volume of subsystem A . The Rényi entropy is analytic around $\chi = 0$ and $M = 1$ and is proportional to the volume and specific heat of free-electron gas [39] $C_A = \rho_A \pi^2/(3\beta_A)$ as [31]

$$\ln s_M(\chi) \approx \frac{V_A C_A}{2} \left(\frac{1}{M - i\chi} - M + i\chi \right). \quad (34)$$

In the limit of zero temperature $\beta_A \rightarrow \infty$, Eq. (34) becomes zero except at $M = i\chi$.

B. Keldysh-generating function

We adopt the replica trick to calculate the information-generating function (15). First, we calculate

$$S_M(\chi) = \text{Tr}_A(\hat{\rho}'_A{}^M \hat{\rho}_{\text{Aeq}}^{-i\chi}) \quad (35a)$$

for a positive integer M and then perform the analytic continuation back to $M \rightarrow 1 - i\xi$. By utilizing expression of the

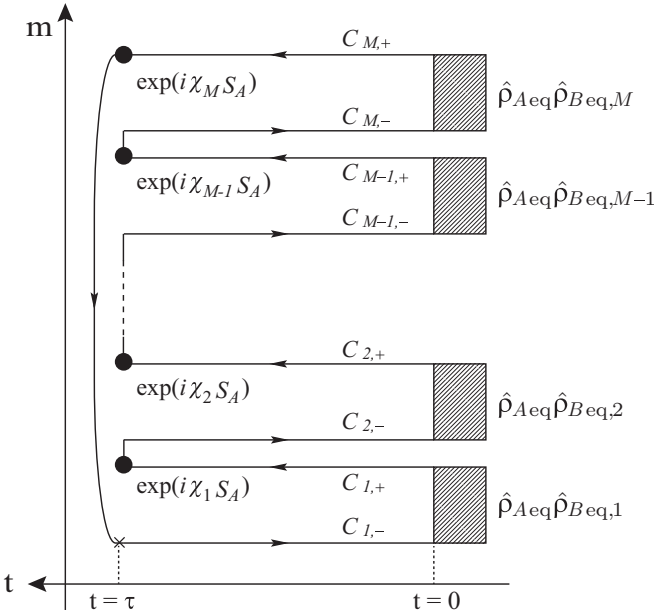


FIG. 2. Multicontour C consisting of M normal Keldysh contours C_1, \dots, C_M . A cross at $t = \tau$ on the lower branch of the first Keldysh contour $C_{1,-}$ represents a starting point. The contour goes to $\hat{\rho}_{\text{Aeq}}\hat{\rho}_{\text{Beq},1}$ at $t = 0$ along $C_{1,-}$ and returns to $t = \tau$ along $C_{1,+}$. Then, it connects to $t = \tau$ on the lower branch of the second Keldysh contour $C_{2,-}$. The contour goes repeatedly until it reaches $t = \tau$ on $C_{M,+}$. Then, it goes back to the starting point $t = \tau$ on $C_{1,-}$. Shaded boxes are M replicas of the initial equilibrium density matrix $\hat{\rho}_{\text{Aeq}}\hat{\rho}_{\text{Beq},m}$ ($m = 1, \dots, M$). Solid circles on $t = \tau_{m+}$ represent operators $\exp(i\chi_m S_A)$.

projection operator (11), the Rényi entropy becomes

$$S_M(\chi) = \left(\frac{\Delta}{2\pi}\right)^{M-1} \int_{-\pi/\Delta}^{\pi/\Delta} d\chi_M \dots d\chi_1 \delta(\chi - \bar{\chi}) \times S_M(\{\chi_j\}), \quad (35b)$$

$$S_M(\{\chi_j\}) = \text{Tr}_A[\hat{\rho}_{\text{Aeq}}^{-i\chi_M} \hat{\rho}_A(\tau) \dots \hat{\rho}_{\text{Aeq}}^{-i\chi_1} \hat{\rho}_A(\tau)], \quad (35c)$$

where $\bar{\chi} = \sum_{j=1}^M \chi_j$. The operator of the local heat quantity (9) includes only the creation and annihilation operators acting locally on subsystem A . In this case, $\hat{\rho}_A(\tau)$ and \hat{Q}_A are, in general, not commutative (Appendix B):

$$[\hat{\rho}_A(\tau), \hat{Q}_A] = \text{Tr}_B(e^{-i\hat{H}\tau} [\hat{\rho}_{\text{Aeq}}\hat{\rho}_{\text{Beq}}, \hat{V} - e^{i\hat{H}\tau}\hat{V}e^{-i\hat{H}\tau}] e^{i\hat{H}\tau}) \neq 0. \quad (36)$$

Therefore, we must deal with multiple integrals over χ_j in Eq. (35b). This situation contrasts with the *local* particle-number constraint [34], in which (under certain conditions) the coherence between sectors of different particle numbers vanishes $[\hat{\rho}_A, \hat{N}_A] = 0$ [see Eq. (26) and Appendix A of Ref. [34]] and thus the M -multiple integral is reduced to a single integral.

Equation (35c) is expressed as the Keldysh partition function defined on a multicontour [31–36]. The multicontour C is a sequence of M normal Keldysh contours C_1, \dots, C_M (Fig. 2). We introduce M replicas of creation and annihilation operators of the subsystem B , $\hat{a}_{Bk}(\hat{a}_{Bk}^\dagger) \rightarrow \hat{a}_{Bk,m}(\hat{a}_{Bk,m}^\dagger)$, living on the m th Keldysh contour C_m ($m = 1, \dots, M$). The

operators of the Hamiltonian and the number of particles of subsystem B are replicated as $\hat{H}_B \rightarrow \hat{H}_{B,m}$ and $\hat{N}_B \rightarrow \hat{N}_{B,m}$, respectively. In addition, the operator of the coupling is replicated as $\hat{V} \rightarrow \hat{V}_m$. Then, the Rényi entropy (35c) is written in the form of the Keldysh partition function

$$S_M(\{\chi_j\}) = \langle \hat{T}_C e^{-i \int_C dt \hat{V}(t) + i \sum_{m=1}^M \chi_m \hat{S}_A(\tau_{m+})} \rangle_M s_M(\bar{\chi}), \quad (37a)$$

where \hat{T}_C is the contour-ordering operator [33,34]. The operators in the interaction picture at time $t_{m\pm}$ on the upper (lower) branch of m th Keldysh contour are, e.g., $V(t_{m\pm})_I = e^{i(\hat{H}_A + \hat{H}_{B,m})t} \hat{V}_m e^{-i(\hat{H}_A + \hat{H}_{B,m})t}$. The average is

$$\langle \hat{O} \rangle_M = \text{Tr}(\hat{O} \hat{\rho}_{\text{Aeq}} \hat{\rho}_{\text{Beq},M} \dots \hat{\rho}_{\text{Aeq}} \hat{\rho}_{\text{Beq},1}) / s_M(\bar{\chi}), \quad (37b)$$

where s_M is the unperturbed part of the Rényi entropy (28). The density matrix of subsystem B is also replicated as $\hat{\rho}_{\text{Beq},m}$. The trace is performed over the Hilbert space of subsystem A and M replicas of subsystem B . The result (37a) is Eq. (46) in Ref. [34] replaced \hat{N}_A with \hat{S}_A . For detailed derivations, see Ref. [34].

C. Multicontour Keldysh Green functions

Here, we illustrate the multicontour Keldysh Green function for a simple model:

$$\hat{H}_r = \epsilon_r \hat{a}_r^\dagger \hat{a}_r \quad (r = A, B). \quad (38)$$

We relegate details to Appendix C and summarize definitions. A multicontour Keldysh Green function of subsystem A is a contour-ordered correlation function of \hat{a}_A^\dagger on $C_{m',s'}$ and \hat{a}_A on $C_{m,s}$:

$$g_A^{\{\chi_j\}}(t_{ms}, t'_{m's'}) = g_A^{\{\chi_j\}, ms, m's'}(t, t') = -i \langle \hat{T}_C \hat{a}_A(t_{ms}) \hat{a}_A^\dagger(t'_{m's'}) e^{i \sum_{j=1}^M \chi_j \hat{S}_A(\tau_{j+})} \rangle_M. \quad (39a)$$

This is a $(ms, m's')$ component of a $2M \times 2M$ Keldysh Green function matrix \mathbf{g}_A [see Eq. (C1) for explicit expressions of components]. It is convenient to introduce the Fourier transform in time:

$$\mathbf{g}_A^{\{\chi_j\}}(\omega) = \int d(t-t') e^{i\omega(t-t')} \mathbf{g}_A^{\{\chi_j\}}(t, t') = \mathbf{U}(\{\delta\chi_j\}, \omega)^\dagger \mathbf{g}_A^{\bar{\chi}}(\omega) \mathbf{U}(\{\delta\chi_j\}, \omega), \quad (39b)$$

which is separated into a matrix $\mathbf{g}_A^{\bar{\chi}}$ depending only on the average of the counting fields $\bar{\chi} = \sum_{m=1}^M \chi_m$ and a diagonal unitary matrix \mathbf{U} depending only on fluctuations $\delta\chi_j = \chi_j - \bar{\chi}/M$ ($j = 1, \dots, M-1$). A $(ms, m's')$ component of the diagonal unitary matrix is

$$[\mathbf{U}]_{ms, m's'} = e^{-i\phi_m(\omega)} \delta_{m, m'} \delta_{s, s'}. \quad (39c)$$

The phase ϕ_m is the accumulation of the fluctuations: $\phi_m(\omega) = \sum_{j=1}^{m-1} \delta\chi_j s_A(\omega)$ for $m = 2, \dots, M$ and $\phi_1(\omega) = 0$. We introduced the dimensionless heat quantity associated with a single-electron excitation $s_A(\omega) = \beta_A(\omega - \mu_A)$. The matrix $\mathbf{g}_A^{\bar{\chi}}(\omega)$ is a block skew-circulant matrix [see Eqs. (C3)–(C6)].

Similarly, a multicontour Keldysh Green function of subsystem B is introduced. It is nonzero only when $\hat{a}_{B,m}$ and $\hat{a}_{B,m'}^\dagger$

are on the same normal Keldysh contour $m = m'$:

$$g_B(t_{ms}, t'_{m's'}) = -i \text{Tr}_{B,m} [T_{C_m} \hat{a}_B(t_{ms})_I \hat{a}_B^\dagger(t'_{m's'})_I \hat{\rho}_{\text{Beq},m}] \delta_{m,m'}. \quad (40)$$

In the following calculations, we will use its Fourier transform in time [see Eqs. (C10) and (C11)].

IV. RESONANT-LEVEL MODEL

We consider the spinless resonant-level model [Fig. 1(b)]. We bipartition the system and regard the left lead as subsystem A and the dot and right lead as subsystem B . The Hamiltonians of the two subsystems are

$$\hat{H}_A = \sum_k \epsilon_{Lk} \hat{a}_{Lk}^\dagger \hat{a}_{Lk}, \quad (41a)$$

$$\hat{H}_B = \sum_k \epsilon_{Rk} \hat{a}_{Rk}^\dagger \hat{a}_{Rk} + \epsilon_D \hat{d}^\dagger \hat{d}, \quad (41b)$$

where \hat{a}_{rk} annihilates an electron with wave number k in the lead r and \hat{d} annihilates an electron in the quantum dot. Here, ϵ_D is the energy of a localized level in the dot and ϵ_{rk} is the energy of the electron in the lead r . The coupling between the two subsystems is described by the tunnel Hamiltonian

$$\hat{V} = \sum_{r=L,R} \sum_k J_r \hat{d}^\dagger \hat{a}_{rk} + \text{H.c.} \quad (41c)$$

The particle-number operators in subsystems A and B are $\hat{N}_A = \hat{N}_L = \sum_k \hat{a}_{Lk}^\dagger \hat{a}_{Lk}$ and $\hat{N}_B = \hat{N}_R + \hat{N}_D = \sum_k \hat{a}_{Rk}^\dagger \hat{a}_{Rk} + \hat{d}^\dagger \hat{d}$, respectively. The inverse temperatures (chemical potentials) of the left and right leads are $\beta_L = \beta_A$ ($\mu_L = \mu_A$) and $\beta_R = \beta_B$ ($\mu_R = \mu_B$). As for the initial isolated dot, one may choose an arbitrary density matrix since, in the steady state, the occupation of the dot level is governed by the electron distribution of the leads and is independent of the initial density matrix of the dot. Therefore, we assume that the initial density matrix of the dot possesses the same form as the equilibrium density matrix (7) and is characterized by two auxiliary parameters, the ‘‘inverse temperature’’ β_D and the ‘‘chemical potential’’ μ_D . This form is convenient since it enables us to utilize the Bloch–De Dominicis theorem (Appendix A of Ref. [33]). As demonstrated in Appendix D, the parameters β_D and μ_D disappear in the course of calculations and the final result (51) is independent of the two parameters.

The Keldysh partition function (37a) can be calculated by exploiting the linked cluster expansion [33,34]. In the limit of long measurement time, the leading contribution is proportional to τ :

$$\ln \frac{S_M(\{\chi_j\})}{S_M(\bar{\chi})} \approx \tau \int \frac{d\omega}{2\pi} \ln \frac{\det[\mathbf{G}_D^{(\chi_j)}(\omega)^{-1}]}{\det[\mathbf{g}_D(\omega)^{-1}]}, \quad (42)$$

where the full Green function matrix of the dot is

$$\mathbf{G}_D^{(\chi_j)^{-1}} = \mathbf{g}_D^{-1} - (\mathbf{1} \otimes \boldsymbol{\tau}_3) \sum_k (J_L^2 U^\dagger \mathbf{g}_{Lk}^\chi U + J_R^2 \mathbf{g}_{Rk}) (\mathbf{1} \otimes \boldsymbol{\tau}_3). \quad (43)$$

Here, \mathbf{g}_{Lk}^χ is obtained from \mathbf{g}_A^χ [Eq. (C3)] by replacing ϵ_A with ϵ_{Lk} . Similarly, $\mathbf{g}_{D(Rk)}$ is obtained from \mathbf{g}_B [Eq. (C10)] by replacing ϵ_B with $\epsilon_{D(Rk)}$. The diagonal unitary matrix U

was introduced in Eq. (39c). Equation (43) can be written as $\mathbf{G}_D^{(\chi_j)^{-1}} = \mathbf{U}^\dagger \mathbf{G}_D^{\bar{\chi}}^{-1} \mathbf{U}$, where

$$\mathbf{G}_D^{\bar{\chi}}^{-1} = \mathbf{g}_D^{-1} - (\mathbf{1} \otimes \boldsymbol{\tau}_3) \sum_k (J_L^2 \mathbf{g}_{Lk}^{\bar{\chi}} + J_R^2 \mathbf{g}_{Rk}) (\mathbf{1} \otimes \boldsymbol{\tau}_3). \quad (44)$$

By exploiting the property of the determinant

$$\det[\mathbf{G}_D^{(\chi_j)^{-1}}] = \det[\mathbf{U}^\dagger \mathbf{G}_D^{\bar{\chi}}^{-1} \mathbf{U}] = \det \mathbf{G}_D^{\bar{\chi}}^{-1}, \quad (45)$$

we observe that the phase $\phi_m(\omega)$ cancels and thus Eq. (42) depends only on the average $\bar{\chi}$. This cancellation originates from the energy conservation in the steady state [40]. It implies that in the steady state, $\hat{\rho}_A$ and \hat{Q}_A commute; see also Sec. VIII B.

Since $\mathbf{g}_{Lk}^{\bar{\chi}}$ is a block skew-circulant matrix, it is block diagonalized by the discrete Fourier transform (C7). Then, Eq. (35b) is calculated as

$$\begin{aligned} \ln \frac{S_M(\chi)}{S_M(\bar{\chi})} &\approx \sum_{\ell=0}^{M-1} \tau \int \frac{d\omega}{2\pi} \ln \frac{\det[\mathcal{G}_D^{\lambda_\ell - \chi_{SA}(\omega)/M}(\omega)^{-1}]}{\det[\mathbf{g}_D(\omega)^{-1}]} \\ &= \tau \sum_{\ell=0}^{M-1} \mathcal{F}_G[\lambda_\ell - \chi_{SA}(\omega)/M], \end{aligned} \quad (46)$$

where the full Green function matrix in the 2×2 normal Keldysh space is

$$\mathcal{G}_D^{\lambda_\ell} = \mathbf{g}_D^{-1} - \boldsymbol{\tau}_3 \sum_k (J_L^2 \mathbf{g}_{Lk}^{\lambda_\ell} + J_R^2 \mathbf{g}_{Rk}) \boldsymbol{\tau}_3. \quad (47)$$

The free Green functions \mathbf{g} are 2×2 matrices [see Eqs. (C8) and (C11)]. The solution to this Dyson equation is given by Eq. (D3) in Appendix D. The function \mathcal{F}_G is related to the scaled cumulant-generating function of the full counting statistics:

$$\begin{aligned} \mathcal{F}_G(\lambda) &= \frac{N_{\text{ch}}}{2\pi} \int d\omega \ln \Omega_{1,\lambda}(\omega), \quad N_{\text{ch}} = 1 \\ \Omega_{M,\lambda}(\omega) &= \frac{\tilde{f}_L^+(\omega)^M + \tilde{f}_L^-(\omega)^M e^{i\lambda}}{\tilde{f}_L^+(\omega)^M + \tilde{f}_L^-(\omega)^M e^{i\lambda}}, \end{aligned} \quad (48)$$

where we subtracted a trivial constant to satisfy the normalization condition $\mathcal{F}_G(0) = 0$. We introduced the effective electron (hole) distribution function $\tilde{f}_L^\pm(\omega) = \mathcal{T}(\omega) f_R^\pm(\omega) + \mathcal{R}(\omega) f_L^\pm(\omega)$, where $\mathcal{T}(\omega)$ is the transmission probability and $\mathcal{R}(\omega) = 1 - \mathcal{T}(\omega)$ is the reflection probability:

$$\mathcal{T}(\omega) = \frac{\Gamma_L \Gamma_R}{(\omega - \epsilon_D)^2 + \Gamma^2/4}, \quad \Gamma = \Gamma_L + \Gamma_R. \quad (49)$$

The coupling strength between the quantum dot and the lead r , $\Gamma_r = 2\pi \sum_k J_r^2 \delta(\omega - \epsilon_{rk})$, is assumed to be energy independent. After we perform the summation over ℓ in Eq. (46) (Appendix E), we obtain

$$\ln \frac{S_M(\chi)}{S_M(\bar{\chi})} \approx \frac{\tau N_{\text{ch}}}{2\pi} \int d\omega \ln \Omega_{M, -\chi_{SA}(\omega)}(\omega). \quad (50)$$

The above results are modifications of those obtained in Refs. [33,34]. Equation (46) is Eq. (64) in Ref. [34]; χ is replaced by $\chi_{SA}(\omega)$. Expressions in Eq. (48) are Eqs. (53) and (54) in Ref. [33]. Technical details can be found in these works.

The order in which the zero-temperature limit and the analytic continuation are taken is important when we consider universal relations associated with the Rényi entropy of order zero [33,34]. Here, we take the zero-temperature limit only

$$\begin{aligned} \ln S_M(X) = & \frac{\tau N_{\text{ch}}}{2\pi} \int_{\mu_A}^{\infty} d\omega \ln[(\mathcal{T}(\omega)f_R^+(\omega))^M e^{iX(\omega-\mu_A)} + (1 - \mathcal{T}(\omega)f_R^+(\omega))^M] \\ & + \frac{\tau N_{\text{ch}}}{2\pi} \int_{-\infty}^{\mu_A} d\omega \ln[(1 - \mathcal{T}(\omega)f_R^-(\omega))^M + (\mathcal{T}(\omega)f_R^-(\omega))^M e^{-iX(\omega-\mu_A)}]. \end{aligned} \quad (51)$$

The two terms on the right-hand side of the equation correspond to the electron and hole contributions. By performing the analytical continuation $M \rightarrow 1 - i\xi$, we obtain the information-generating function. We check that Eq. (51) satisfies

$$\ln S_1(X = 0) = 0, \quad (52)$$

and thus the joint probability distribution function is properly normalized to 1 [see Eq. (27)].

V. OPTIMUM CAPACITY

A. Averages

From Eq. (51), by exploiting Eq. (18), the average of the self-information is evaluated:

$$\begin{aligned} \langle\langle I'_A \rangle\rangle = & \frac{\tau N_{\text{ch}}}{2\pi} \int_{\mu_A}^{\infty} d\omega H_2(\mathcal{T}(\omega)f_R^+(\omega)) \\ & + \frac{\tau N_{\text{ch}}}{2\pi} \int_{-\infty}^{\mu_A} d\omega H_2(\mathcal{T}(\omega)f_R^-(\omega)), \end{aligned} \quad (53)$$

where we introduced the binary entropy $H_2(x) = -x \ln x - (1-x) \ln(1-x)$. The first and second terms on the right-hand side correspond to electron and hole contributions, respectively. The integrand $H_2(\mathcal{T}f_R^\pm)$ is the entropy of the receiver side. It corresponds to $H(B)$ of Eq. (21) in Ref. [14] and Eq. (12) of Ref. [12]. The average heat quantity in the left reservoir is

$$\langle\langle Q_A \rangle\rangle = \frac{\tau N_{\text{ch}}}{2\pi} \int d\omega (\omega - \mu_A) \mathcal{T}(\omega) [f_R^+(\omega) - f_L^+(\omega)], \quad (54)$$

which corresponds to the average signal power, Eq. (15) in Ref. [14].

B. Optimum capacity and integer partitions

Let us take $M \rightarrow 0$ of Eq. (51) while keeping the inverse temperature β_B finite. For $\mathcal{T}(\omega) > 0$, $(\mathcal{T}f_R^\pm)^0 = (\mathcal{R} + \mathcal{T}f_R^\pm)^0 = 1$. For $\mathcal{T}(\omega) = 0$, $(\mathcal{T}f_R^\pm)^0 = 0$, and $(\mathcal{R} + \mathcal{T}f_R^\pm)^0 = 1$. Therefore, in this limit, Eq. (51) is independent of the details of the setup and depends only on the statistics of particles.

We consider the band-limited channel: we introduce a finite bandwidth, i.e., a high-frequency cutoff ω_{max} and a low-frequency cutoff, or a gap, $\omega_{\text{min}} > 0$. As is observed from Eq. (51), electrons ($\omega > \mu_A$) and holes ($\omega < \mu_A$) contribute in the same way. Therefore, in the following, when only electrons contribute, i.e., $\omega_{\text{min}} < \omega < \omega_{\text{max}}$, we set $N_{\text{ch}} = \frac{1}{2}$.

for subsystem A, $\beta_A \rightarrow \infty$, while keeping M as a positive integer and the counting field $\beta_A \chi = X$ finite. By setting $f_L^+(\omega) = \theta(\mu_A - \omega)$, which is the Heaviside step function, Eq. (50) becomes

When electrons and holes contribute, i.e., $\omega_{\text{min}} < |\omega| < \omega_{\text{max}}$, we set $N_{\text{ch}} = 1$. The Rényi entropy of order zero is

$$\begin{aligned} \ln S_0(X = \lambda/\Delta E) = & \frac{1}{\Delta E} \int_{\omega_{\text{min}}}^{\omega_{\text{max}}} d\omega \ln(e^{iX\omega} + 1) \\ = & \int_{j_{\text{min}}}^{j_{\text{max}}} dj \ln(1 + e^{i\lambda j}), \end{aligned} \quad (55)$$

where $j = \omega/\Delta E$. The energy resolution is $\Delta E = h/(2N_{\text{ch}}\tau)$ [see Eq. (22)]. It is an approximation of the logarithm of the generating function for partitions [13]: $\prod_{j \in \mathcal{S}} (1 + e^{i\lambda j}) = \sum_{n \geq 0} p(n|\text{distinct parts in } \mathcal{S}) e^{in\lambda}$, where $\mathcal{S} = \{j_{\text{min}}, j_{\text{min}} + 1, \dots, j_{\text{max}}\}$. The *partition function* [13] $p(n|\text{distinct parts in } \mathcal{S})$ stands for the number of *integer partitions* of a given integer n into distinct elements of the set \mathcal{S} . The *integer partition* of n is a way of writing n as the sum of positive integers. By exploiting Eq. (22), we obtain

$$\langle e^j \rangle_{Q_A} \approx p(Q_A/\Delta E|\text{distinct parts in } \mathcal{S}), \quad (56)$$

which is $\exp[\tau C_{\text{opt}}(P_A)]$ according to the previous quantum information theory approach in Ref. [10] [see Eq. (90c) in Sec. VIII].

The result presented above verifies our main claim, Eq. (5). However, precisely speaking, there are differences. The previous works [9,10] treated dispersionless channels. Our result is derived from a microscopic Hamiltonian and can be extended to channels with arbitrary dispersion. We present more detailed comparisons in Sec. VIII.

The integral in Eq. (55) can be done analytically:

$$\ln S_0(X = \lambda/\Delta E) = \frac{\text{Li}_2(-e^{i\lambda j_{\text{min}}}) - \text{Li}_2(-e^{i\lambda j_{\text{max}}})}{i\lambda}, \quad (57)$$

where the dilogarithm function is

$$\text{Li}_2(x) = \sum_{k=1}^{\infty} \frac{x^k}{k^2} = \int_x^0 dz \frac{\ln(1-z)}{z}. \quad (58)$$

For the narrow-band case, when the bandwidth $2\pi B = \omega_{\text{max}} - \omega_{\text{min}}$ and the frequency $2\pi f = (\omega_{\text{max}} + \omega_{\text{min}})/2$ satisfy $B \ll f$, the generating function is approximately $\ln S_0(X = \lambda/\Delta E) \approx 2\tau N_{\text{ch}} B \ln(1 + e^{i2\tau N_{\text{ch}} f \lambda})$. Then, by substituting it into Eqs. (22) and (5), we obtain

$$C_{\text{opt}}(P_A) \approx 2N_{\text{ch}} B H_2(P_A/(2N_{\text{ch}} h f B)). \quad (59a)$$

In the particlelike regime, $P_A \ll 2N_{\text{ch}} h f B$, where the signal power is small and the particle nature of an electron is

prominent:

$$C_{\text{opt}}(P_A) \approx \frac{P_A}{hf} \ln \frac{2N_{\text{ch}}hfB}{P_A}. \quad (59b)$$

Here, $P_A/(hf)$ is the rate of transmission of signal quanta. The argument of the logarithm $2N_{\text{ch}}hfB/P_A$ means the maximum number of distinguishable modes per signal quantum. For $N_{\text{ch}} = \frac{1}{2}$, the expression is formally compatible with Eq. (2.22) in Ref. [9] that was obtained for bosons.

For the fermionic band-limited channel, the power of the signal is bounded from above. Let us set $\omega_{\text{min}} = 0$. The maximum of the heat quantity is

$$\frac{Q_{A \text{ max}}}{\Delta E} = \lim_{i\lambda \rightarrow \infty} \frac{\ln S_0(X = \lambda/\Delta E)}{i\lambda} = \frac{j_{\text{max}}^2}{2}, \quad (60a)$$

where we utilized the Legendre duality [37] and the fact that a rare event associated with the maximum is realized in the limit of $i\lambda \rightarrow \infty$. The maximum power is

$$P_{A \text{ max}} = \frac{Q_{A \text{ max}}}{\tau} = \frac{2N_{\text{ch}}}{h} \int_0^{\omega_{\text{max}}} \omega d\omega, \quad (60b)$$

which is the Landauer formula of heat current for perfect transmission.

Let us turn our attention to the wide-band channel $j_{\text{max}} \rightarrow \infty$. As long as the inverse Fourier transform is performed within the saddle-point approximation [see Eq. (22)], it is sufficient to analyze the generating function (55) for pure imaginary λ . The integral in Eq. (55) can be done for $i\lambda < 0$ and we obtain

$$\ln S_0(X = \lambda/\Delta E) \approx -\frac{\pi^2}{12i\lambda}. \quad (61a)$$

Then, by substituting it into Eq. (22) and by using Eq. (5), we reproduce the optimum capacity of the wide-band channel (1):

$$C_{\text{opt}}(P_A) \approx \frac{\pi}{\tau} \sqrt{\frac{Q_A/\Delta E}{3}} = C_{\text{WB}}(P_A), \quad (61b)$$

where $P_A > 0$.

Figure 3 shows the optimum capacity as a function of the signal power of the band-limited channel without the gap $\omega_{\text{min}} = 0$. The horizontal axis is the heat quantity normalized by ΔE , $Q_A/\Delta E = \tau^2 N_{\text{ch}} P_A/\pi$. For a small cutoff energy ($j_{\text{max}} = N_{\text{ch}}\tau\omega_{\text{max}}/\pi = 5$), the curve is well fitted by the optimum capacity of the narrow-band channel (59a) indicated by the dotted-dashed line. The signal power P_A is bounded from above and the maximum is given by Eq. (60b). The dashed line indicates the optimum capacity of the wide-band channel (61b). With the increase in cutoff energy ω_{max} , the curve approaches the dashed line.

As we noted, if we change the order in which the zero-temperature limit and the analytic continuation are taken, the result mentioned above changes [33,34]. When we set $M = 0$ while keeping the inverse temperature β_A finite, since $(f_L^\pm)^0 = (\tilde{f}_L^\pm)^0 = 1$, Eq. (50) becomes $S_0(\chi) = s_0(\chi)$ [see Eq. (34)]. By taking the limit of zero temperature $\beta_A \rightarrow \infty$

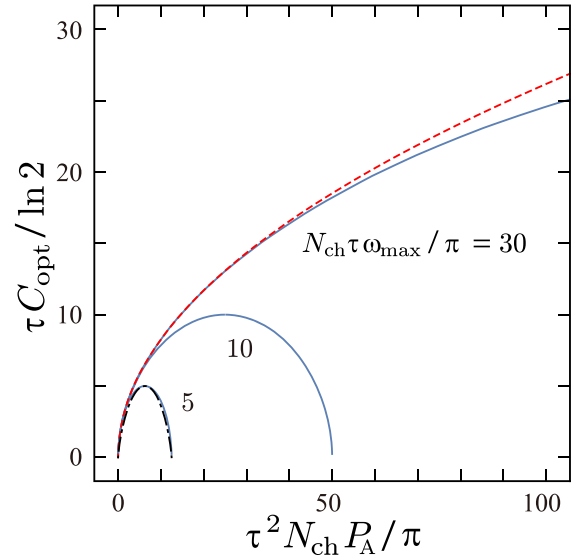


FIG. 3. The optimum capacity as a function of signal power P_A for various bandwidths ω_{max} (the gap is zero $\omega_{\text{min}} = 0$). The dotted-dashed line indicates the optimum capacity of the narrow-band channel (59a). The dashed line indicates the optimum capacity of the wide-band channel (61b).

while keeping $X = \beta_A \chi$ finite, we obtain

$$\ln S_0(X) = -\frac{V_A \gamma_A}{2iX} \quad (iX < 0), \quad (62a)$$

where $\gamma_A = C_A \beta_A = \pi^2 \rho_A/3$ is the electronic specific-heat coefficient. Then, the size of the Fock subspace is estimated as

$$\ln S_{0,Q_A} \approx \sqrt{2V_A \gamma_A Q_A}, \quad (62b)$$

which may look similar to τC_{opt} [Eq. (61b)]. However, it is not universal and depends on the setup; in order to obtain this form, we assume that the DOS is energy independent in Eq. (34). Moreover, Eq. (62b) depends not on τ but on V_A and thus is related to bulk states.

VI. PROBABILITY DISTRIBUTIONS

A. Narrow-band channel

For a narrow-band channel, $B \ll f$, with perfect transmission $\mathcal{T}(\omega) = \theta(\omega_{\text{max}} - \omega)\theta(\omega - \omega_{\text{min}})$, the Rényi entropy (51) becomes

$$\ln S_M(X) = \tau 2N_{\text{ch}} B \ln[f_R^+(hf)^M e^{iXhf} + f_R^-(hf)^M]. \quad (63a)$$

Then, by performing the inverse Fourier transform of Eq. (15) within the saddle-point approximation, we obtain

$$\ln S_M(Q_A) = \min_{iX \in \mathbb{R}} [\ln S_M(X) - iX Q_A] \quad (63b)$$

$$= -M\tau 2N_{\text{ch}} B D(p||q) + (1-M) \times \tau 2N_{\text{ch}} B H_2(P_A/(2N_{\text{ch}}hfB)). \quad (63c)$$

Here, $D(p||q) = \sum_j p_j \ln(p_j/q_j)$ is the relative entropy between the distribution $p = (P_A/(2N_{\text{ch}}hfB), 1 - P_A/(2N_{\text{ch}}hfB))$ and $q = (f_R^+(hf), f_R^-(hf))$, which measures

the difference between the two distributions p and q . After the inverse Fourier transform (16a), we obtain the joint probability distribution, which is the delta distribution:

$$P(I'_A, Q_A) = e^{-\tau 2N_{\text{ch}} B D(p||q)} \delta(I'_A - \tau 2N_{\text{ch}} B (H_2 + D(p||q))). \quad (64)$$

Here, $\tau 2N_{\text{ch}} B$ and $\tau P_A/(hf)$ are interpreted, respectively, as the number of modes and the number of signal quanta, i.e., electrons transmitted to the receiver side. When the ratio between these numbers is compatible with the initial electron distribution probability $f_R^+(hf) = P_A/(2N_{\text{ch}} hfB)$, the relative entropy takes its minimum value $D(p||q) = 0$. In this case, the transmitted self-information is always $I'_A = \tau 2N_{\text{ch}} B H_2(f_R^+(hf))$.

The information-generating function (19) can be derived from Eq. (63c): $\ln S_{1-i\xi, Q_A} = i\xi \tau 2N_{\text{ch}} B H_2(P_A/(2N_{\text{ch}} hfB))$. Then, the conditional self-information is delta distributed as

$$P_{Q_A}(J) = \delta(J - \tau 2N_{\text{ch}} B H_2(P_A/(2N_{\text{ch}} hfB))). \quad (65)$$

It is independent of the electron distribution probability. Therefore, the conditional self-information is always

$$J = \tau 2N_{\text{ch}} B H_2(P_A/(2N_{\text{ch}} hfB)) \approx \ln \left(\frac{\tau 2N_{\text{ch}} B}{\tau P_A/(hf)} \right), \quad (66)$$

which is the number of possible ways to locate transmitted electrons in available scattering states in subsystem A. In order to obtain the last expression in Eq. (66), we utilized the approximate form of the binomial coefficient, $\ln \binom{N}{n} \approx N H_2(n/N)$, which is obtained by applying Stirling's approximation $\ln n! \approx n \ln(n/e)$ for $n \gg 1$.

B. Wide-band channel

Let us consider the wide-band quantum channel $\omega_{\text{max}} \rightarrow \infty$, $\omega_{\text{min}} = 0$, and $\mathcal{T}(\omega) = 1$. The Rényi entropy (51) is analytic around $X = 0$ and $M = 1$:

$$\ln S_M(X) = \tau P_\beta \beta_B^2 \left(\frac{1}{M\beta_B - iX} - \frac{M}{\beta_B} \right) + \tau \frac{P_\mu}{2} \frac{M\beta_B iX}{M\beta_B - iX}, \quad (67)$$

where $P_\mu = N_{\text{ch}} g_0^{\text{el}} (\mu_B - \mu_A)^2$ is the rate of Joule heat generation and $P_\beta = N_{\text{ch}} g_0 / \beta_B$ is the heat current emitted from subsystem B, the right reservoir. The coefficients are the conductance quantum $g_0^{\text{el}} = 1/(2\pi)$ and the thermal conductance quantum [41] $g_0 = \pi/6 \times (\beta_A^{-1} + \beta_B^{-1})/2 = \pi/(12\beta_B)$.

Averages are obtained by performing the derivative (18) as

$$\langle\langle I'_A \rangle\rangle = 2\tau \beta_B P_\beta, \quad \langle\langle Q_A \rangle\rangle = \tau (P_\beta + P_\mu/2). \quad (68)$$

When the chemical potential bias is absent, $\mu_A = \mu_B$, we can eliminate β_B and obtain

$$\frac{\langle\langle I'_A \rangle\rangle}{\tau} = \sqrt{\frac{\pi}{3} N_{\text{ch}} \frac{\langle\langle Q_A \rangle\rangle}{\tau}} = C_{\text{WB}}(\langle\langle Q_A \rangle\rangle/\tau), \quad (69)$$

which is the optimum capacity of the wide-band channel (1). The above derivation follows previous approaches in Refs. [5,8]. The second cumulant, variances, and cross

correlations are

$$\langle\langle I'^2_A \rangle\rangle = \beta_B \langle\langle I'_A Q_A \rangle\rangle = \langle\langle I'_A \rangle\rangle, \quad \langle\langle Q^2_A \rangle\rangle = 2\langle\langle Q_A \rangle\rangle / \beta_B. \quad (70a)$$

Since the cross correlation is positive, the correlation coefficient is also positive:

$$r = \frac{\langle\langle I'_A Q_A \rangle\rangle}{\sqrt{\langle\langle I'^2_A \rangle\rangle \langle\langle Q^2_A \rangle\rangle}} = \sqrt{\frac{2P_\beta}{2P_\beta + P_\mu}} > 0. \quad (70b)$$

The correlation coefficient r ranges from -1 to 1 and measures the degree of linear correlation between the two fluctuating variables I'_A and Q_A . From this relation, we can see that when the chemical potential bias is absent, there is a perfect positive linear correlation $r = 1$, which means that there is a one-to-one correspondence between the self-information content and the heat quantity.

1. Conditional self-information

Let us calculate the probability distribution of the conditional self-information. First, we perform the inverse Fourier transform of Eq. (67) within the saddle-point approximation

$$\ln S_M(Q_A) = \tau C_{\text{WB}} \sqrt{1 + M^2 P_\mu / (2P_\beta)} - \tau \beta_B M (P_\beta + P_\mu/2 + P_A). \quad (71a)$$

Then, the Rényi entropy associated with the probability distribution of the conditional self-information (19) becomes

$$\ln S_{M, Q_A} = \tau C_{\text{WB}} (\sqrt{1 + (r^{-2} - 1)M^2} - M r^{-1}). \quad (71b)$$

Finally, the probability distribution is obtained by the inverse Fourier transform within the saddle-point approximation

$$\ln P_{Q_A}(J) = \min_{i\xi \in \mathbb{R}} (\ln S_{1-i\xi, Q_A} - i\xi J) \quad (71c)$$

$$= \tau C_{\text{WB}} \sqrt{1 - \frac{[1 - rJ/(\tau C_{\text{WB}})]^2}{1 - r^2}} - J. \quad (71d)$$

Figure 4(a) shows the Rényi entropy (71b) for various values of the correlation coefficient. We observe that at $M = 0$, i.e., $i\xi = 1$, all curves intersect. Equation (71b) satisfies the universal relation providing the optimum capacity [see Eqs. (5) and (21)] as

$$\ln S_{0, Q_A} = \tau C_{\text{WB}}. \quad (72)$$

Figure 4(b) shows the conditional probability distribution function (71d). The vertical and horizontal axes are normalized by τC_{WB} . The curves are tilted semiellipses and depend only on the correlation coefficient r . The maximum (minimum) is

$$J_{\text{max(min)}} = \lim_{M \rightarrow \mp\infty} \frac{\ln S_{M, Q_A}}{1 - M} = \tau C_{\text{WB}} (r^{-1} \pm \sqrt{r^{-2} - 1}). \quad (73)$$

Here, we utilized the Legendre duality [37] of Eq. (71c) and the fact that a rare event associated with maximum

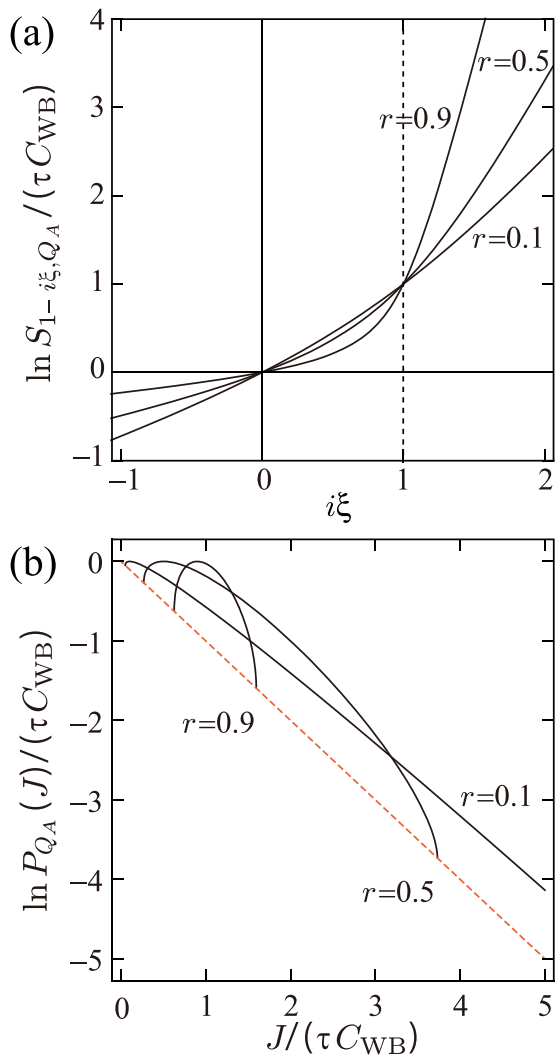


FIG. 4. (a) Information-generating function for wide-band channel. Curves are for a nearly perfectly linearly correlated case ($r = 0.9$), for an intermediate case ($r = 0.5$), and for a nearly uncorrelated case ($r = 0.1$). A vertical dotted line indicates the point $M = 0$, where the universal relation (72) is satisfied. (b) Probability distributions of the conditional self-information content. A dashed line corresponds to the exponential distribution (74b).

(minimum) J is realized in the limit of $M \rightarrow \mp\infty$. From Eq. (73), the width of the distribution is obtained as $J_{\max} - J_{\min} = 2\sqrt{r^2 - 1}$. The width becomes narrower when the two quantities are correlated, as we observe in Fig. 4(b). For the perfect correlation $r = 1$, the delta distribution

$$P_{Q_A}(J) = \delta(J - \tau C_{WB}) \quad (74a)$$

is realized. For the uncorrelated case $r \rightarrow 0$, the exponential distribution [dashed line in Fig. 4(b)]

$$P_{Q_A}(J) \approx e^{-J} \quad (74b)$$

is approached.

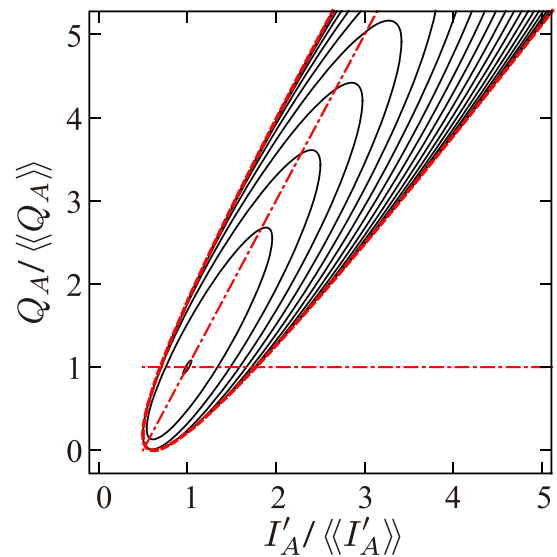


FIG. 5. Contour plot of the logarithm of joint probability distribution function of self-information content and heat quantity for wide-band channel. A thick dotted line indicates the boundary of support [Eq. (77)]. The correlation coefficient is $r = 0.9$. The contour interval is $\langle\langle I'_A \rangle\rangle/4$. Two dotted-dashed lines indicate Eqs. (79a) and (79b).

2. Joint probability distribution

The joint probability distribution function is obtained from Eq. (71a) by applying Eq. (16b) as

$$\begin{aligned} \ln P(I'_A, Q_A) &= \min_{M \in \mathbb{R}} [\ln S_M(Q_A) + M I'_A] - I'_A \quad (75) \\ &= [4\tau\beta_B P_\beta (\tau\beta_B P_\beta + \delta I'_A) - 2P_\beta/P_\mu \\ &\quad \times (\beta_B \delta Q_A - \delta I'_A)^2]^{1/2} - I'_A, \quad (76) \end{aligned}$$

where we introduced $\delta I'_A = I'_A - \langle\langle I'_A \rangle\rangle$ and $\delta Q_A = Q_A - \langle\langle Q_A \rangle\rangle$. Figure 5 is a contour plot of the logarithm of joint probability distribution for $r = 0.9$. The maximum is $\ln P(\langle\langle I'_A \rangle\rangle, \langle\langle Q_A \rangle\rangle) = 0$. A thick dotted line indicates the boundary of support:

$$\frac{\delta Q_A}{\langle\langle Q_A \rangle\rangle} = 2r^2 \left[\frac{\delta I'_A}{\langle\langle I'_A \rangle\rangle} \pm \sqrt{2 \left(\frac{1}{r^2} - 1 \right) \frac{\delta I'_A}{\langle\langle I'_A \rangle\rangle}} \right]. \quad (77)$$

The self-information content is bounded from below and the minimum is half of the average self-information

$$I'_{A\min} = \langle\langle I'_A \rangle\rangle/2. \quad (78)$$

As we observe in Eq. (77), the width of the distribution vanishes in the perfectly linearly correlated case $r = 1$, i.e., $\mu_A = \mu_B$. The boundary of support shrinks to

$$\frac{\delta Q_A}{\langle\langle Q_A \rangle\rangle} = 2 \frac{\delta I'_A}{\langle\langle I'_A \rangle\rangle}, \quad (79a)$$

i.e., the fluctuations satisfy $\delta I'_A = \beta_B \delta Q_A$. Here, we note that the entropy and average heat (68) satisfy $\langle\langle I'_A \rangle\rangle = 2\beta_B \langle\langle Q_A \rangle\rangle > \beta_B \langle\langle Q_A \rangle\rangle$, which implies the irreversible nature of the heat transport process [10]. For $r \neq 1$, although there is no one-to-one correspondence between the two quantities, we may

consider that the two quantities are approximately related as $Q_A/\langle\langle Q_A \rangle\rangle \propto 2r^2 I'_A/\langle\langle I'_A \rangle\rangle$. In the limit of uncorrelated case $r \rightarrow 0$, which corresponds to $P_\beta/P_\mu \rightarrow 0$, Eq. (77) becomes

$$\frac{\delta Q_A}{\langle\langle Q_A \rangle\rangle} \rightarrow 0. \quad (79b)$$

In Fig. 5, Eqs. (79a) and (79b) are indicated by dotted-dashed lines.

C. Short summary of Secs. V and VI

In Secs. V and VI, we provided rather detailed derivations. Here, we summarize relevant results in these two sections:

(i) The Rényi entropy of order zero is related to the generating function of integer partitions:

$$S_0(X = \lambda/\Delta E) \approx \prod_{j \in S} (1 + e^{i\lambda j}), \quad (55)$$

where $S = \{j_{\min}, \dots, j_{\max}\}$ and $j = \omega/\Delta E$ is assumed to be integers. The energy resolution $\Delta E = h/(2N_{\text{ch}}\tau)$ is due to the energy-time uncertainty relation. The expression is independent of details of the mesoscopic quantum electric conductor and only depends on the statistics of particles and the bandwidth.

The optimum capacity for the narrow-band case is

$$C_{\text{NB}}(P_A) = 2N_{\text{ch}}B H_2(P_A/(2N_{\text{ch}}hfB)), \quad (59a)$$

where $H_2(x) = -x \ln x - (1-x) \ln(1-x)$ is the binary entropy. Here, $\tau 2N_{\text{ch}}B$ and $\tau P_A/(hf)$ are the number of modes and the number of signal quanta. Then, $e^{\tau C_{\text{NB}}}$ is regarded as the number of possible ways to distribute signal quanta into available modes.

The optimum capacity for the wide-band case is

$$C_{\text{WB}}(P_A) = \frac{\pi}{\tau} \sqrt{\frac{Q_A/\Delta E}{3}}. \quad (61b)$$

The above-mentioned results derived systematically from the Rényi entropy (51) based on the microscopic Hamiltonian reproduce previous theories (see Refs. [9,10]).

(ii) The conditional self-information for the narrow-band case is delta distributed as

$$P_{Q_A}(J) = \delta(J - \tau C_{\text{NB}}(P_A)). \quad (65)$$

Thus, the conditional self-information does not fluctuate.

For the wide-band channel,

$$\ln P_{Q_A}(J) = \tau C_{\text{WB}} \sqrt{1 - \frac{[1 - rJ/(\tau C_{\text{WB}})]^2}{1 - r^2}} - J, \quad (71d)$$

which depends on the correlation coefficient

$$r = \frac{\langle\langle I'_A Q_A \rangle\rangle}{\sqrt{\langle\langle I'^2_A \rangle\rangle \langle\langle Q^2_A \rangle\rangle}} = \sqrt{\frac{\langle\langle I'_A \rangle\rangle}{2\beta_B \langle\langle Q_A \rangle\rangle}}. \quad (70b)$$

It measures how much two variables I'_A and Q_A are linearly correlated and satisfies $0 \leq r \leq 1$. For $r = 1$, the two variables are perfectly linearly correlated and there is one-to-one correspondence between the two quantities. It is realized when the chemical potential bias is absent, $\mu_A = \mu_B$, and the averages of self-information and heat quantity satisfy $\langle\langle I'_A \rangle\rangle =$

$2\beta_B \langle\langle Q_A \rangle\rangle = \tau N_{\text{ch}} \pi / (6\beta_B)$. In this case, Eq. (71d) is reduced to the delta distribution (74a), $P_{Q_A}(J) = \delta(J - \tau C_{\text{WB}})$. When the chemical potential bias is much larger than the temperature bias $|\mu_B - \mu_A| \gg \beta_B^{-1}$, the two quantities become uncorrelated, $r \rightarrow 0$. In this case, Eq. (71d) becomes the exponential distribution $P_{Q_A}(J) \approx e^{-J}$ [Eq. (74b)].

VII. RESONANT TUNNELING AND COULOMB INTERACTION

A. Energy-dependent transmission probability

In this section, we consider the resonant tunneling condition $\Gamma_L = \Gamma_R$ and $\mu_A = \epsilon_D = 0$, where the transmission probability is

$$\mathcal{T}(\omega) = \frac{1}{1 + 4(\omega/\Gamma)^2}. \quad (80)$$

Figure 6 is a contour plot of the logarithm of joint probability distribution of self-information content and heat quantity obtained by numerically solving Eqs. (17) and (51). In this figure, the voltage difference is small $\mu_B = 0.01\Gamma$ and the temperature of the subsystem B is comparable to the level broadening $\beta_B \Gamma = 1$. A dotted-dashed line indicates the boundary of support for the wide-band channel (77), i.e., the result when $\mathcal{T} = 1$, which implies a perfect linear correlation $I'_A \approx \beta_B Q_A$ [Eq. (79a)]. We checked that the perfect linear correlation is approached when the temperature is low $\beta_B \Gamma \ll 1$. In Fig. 6, since the temperature is comparable to the level broadening, the perfect linear correlation is spoiled.

A dotted line indicates the minimum self-information content for a given heat content. It is almost parallel to the

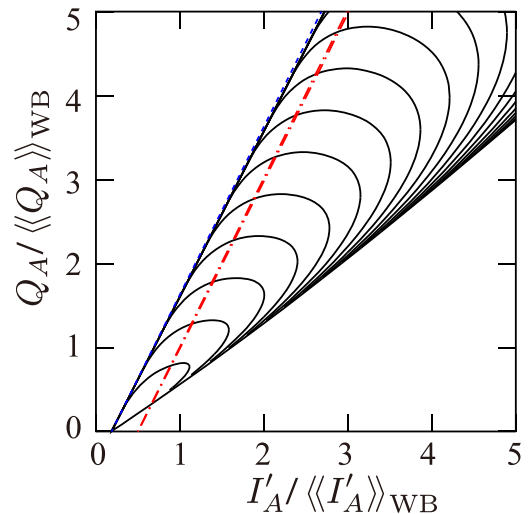


FIG. 6. Contour plot of the logarithm of joint probability distribution function of self-information content and heat quantity close to the resonant tunneling condition. The contour interval is $\langle\langle I'_A \rangle\rangle_{\text{WB}}/4$. A dotted line indicates Eq. (81c). A dotted-dashed line is the boundary of support for the wide-band channel (77). Axes are normalized by the corresponding values of the wide-band channel $\langle\langle I'_A \rangle\rangle_{\text{WB}}$ and $\langle\langle Q_A \rangle\rangle_{\text{WB}}$ [Eqs. (68)]. The average values are $\langle\langle I'_A \rangle\rangle = 0.371 \langle\langle I'_A \rangle\rangle_{\text{WB}}$ and $\langle\langle Q_A \rangle\rangle = 0.139 \langle\langle Q_A \rangle\rangle_{\text{WB}}$. Parameters: $\beta_R \Gamma = 1$, $\mu_R = 0.01\Gamma$, and $\omega_{\text{max}} = 10^3 \Gamma$.

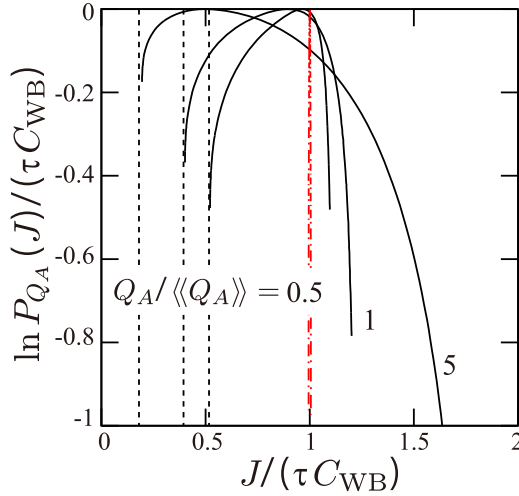


FIG. 7. Probability distribution of conditional self-information close to the resonant tunneling condition. Curves are for various values of heat quantity $Q_A/\langle\langle Q_A \rangle\rangle = 0.5, 1, \text{ and } 5$. A dotted-dashed line indicates the result of the wide-band channel (71d). Dotted lines indicate the minimum of conditional self-information, Eq. (82). The parameters are the same as those in Fig. 6.

dotted-dashed line. The minimum can be estimated in the following. For $M \rightarrow \infty$, the Rényi entropy (51) is approximately

$$\ln S_M(X) \approx MI_m + \tau \frac{\pi}{12} \frac{1}{iX - \beta_B M} \quad (iX < \beta_B M), \quad (81a)$$

$$I_m = \frac{\tau}{\pi} \int_0^\infty d\omega \ln[1 - \mathcal{T}(\omega) f_R^+(\omega)]. \quad (81b)$$

Then, after a few steps of calculations, the minimum is obtained as

$$I'_{A\min} = I_m + \tau \beta_B P_A, \quad (81c)$$

where we used the Legendre duality $I'_{A\min} = \lim_{i\xi \rightarrow -\infty} \ln S_{1-i\xi}(Q_A)/(i\xi)$.

Figure 7 shows the probability distribution of conditional self-information for various values of heat quantity. A dotted-dashed line indicates the result of the wide-band

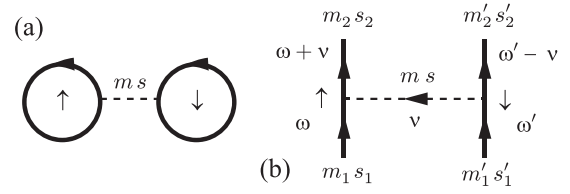


FIG. 8. Diagrams correspond to (a) the Hartree term and (b) the bare interaction vertex. Thick solid lines correspond to the full Green function matrix, Eq. (43). Dotted lines indicate the Coulomb interaction.

channel (71d). The vertical and horizontal axes are normalized by the optimum capacity of the wide-band channel. With an increase in signal power, the peak position shifts leftward, which means that the transmitted information decreases as compared with that of the wide-band channel. At the same time, the width increases, which means that the number of typical sequences decreases. Dotted lines indicate the minimum of conditional self-information corresponding to the dotted line in Fig. 6. The minimum in Fig. 6 and that in Fig. 7 are related as we can deduce from Eq. (13);

$$J_{\min} = I'_{A\min} + \ln P(S_A). \quad (82)$$

B. Coulomb interaction

Here, we discuss the effect of the onsite Coulomb interaction. For this purpose, we adopt the same model in Ref. [33]. Namely, we introduce the spin degree of freedom $\hat{a}_{rk} \rightarrow \hat{a}_{rk\sigma}$ and $\hat{d} \rightarrow \hat{d}_\sigma$ ($\sigma = \uparrow, \downarrow$). The onsite Coulomb interaction is included in the Hamiltonian of subsystem B:

$$\hat{H}_B = \sum_{k\sigma} \epsilon_{Rk} \hat{a}_{Rk\sigma}^\dagger \hat{a}_{Rk\sigma} + \sum_{\sigma} \epsilon_D \hat{d}_\sigma^\dagger \hat{d}_\sigma + U \hat{d}_\uparrow^\dagger \hat{d}_\downarrow^\dagger \hat{d}_\downarrow \hat{d}_\uparrow. \quad (83)$$

Because of the spin degree of freedom, the number of channels is doubled $N_{\text{ch}} = 2$.

We perform the perturbative expansion of the Keldysh partition function [33] (37a) in powers of the Coulomb interaction U . The zeroth-order contribution is Eq. (51). The Hartree term, the first-order contribution, is depicted in Fig. 8 (a):

$$\begin{aligned} iU \sum_{m=1}^M \sum_{s=\pm} s \int_0^\tau dt G_D^{\{X_j\}}(t_{ms}, t_{ms}) G_D^{\{X_j\}}(t_{ms}, t_{ms}) &= iUM\tau \sum_{s=\pm} s \int_0^\tau dt (G_D^{\{X_j\}}(t_{ms}, t_{ms}))^2 \\ &= iUM\tau \sum_{s=\pm} s \left(\int \frac{d\omega}{2\pi} [U^\dagger G_D^{\bar{X}}(\omega) U]_{ms,ms} \right)^2 = \tau 2UMn_{M,\bar{X},q} \delta n_{M,\bar{X}}. \end{aligned} \quad (84)$$

Since $[U^\dagger G_D^{\bar{X}} U]_{ms,ms} = [G_D^{\bar{X}}]_{ms,ms}$, the result is independent of the phase ϕ_m . The classical and quantum components of electron occupancy inside the dot are calculated by using the local Green function matrix (D8):

$$\delta n_{M,\bar{X}} = \int \frac{d\omega}{2\pi} \frac{G_D^{\bar{X},m+,m+}(\omega) + G_D^{\bar{X},m-,m-}(\omega)}{2i} = \int_{-\omega_{\max}}^{\omega_{\max}} d\omega \left(1 - \frac{1}{M} \frac{\partial_{\epsilon_D} \ln \Omega_{M,-\bar{X}} S_A(\omega)(\omega)}{\partial_{\epsilon_D} \ln \rho(\omega)} \right) \rho(\omega) \sum_r \frac{\Gamma_r}{\Gamma} [f_r^+(\omega) - 1/2], \quad (85)$$

$$n_{M,\bar{X},q} = \int_{-\omega_{\max}}^{\omega_{\max}} \frac{d\omega}{2\pi} [G_D^{\bar{X},m-,m-}(\omega) - G_D^{\bar{X},m+,m+}(\omega)] = \partial_{\epsilon_D} \ln S_M(\bar{X}) / (MN_{\text{ch}} \tau), \quad (86)$$

where we introduced the cutoff energy ω_{\max} . Since $\delta n_{0,\bar{\chi}}$ and $n_{0,\bar{\chi},q}$ are finite, we confirm that the Hartree term vanishes when we take the limit $M \rightarrow 0$. Therefore, the optimum capacity is not affected by the weak Coulomb interaction.

As we mentioned, the first-order contribution is independent of the phase ϕ_m . The same is true for any closed diagram. Let us analyze the interaction vertex on the s branch of the m th Keldysh contour [Fig. 8(b)]:

$$\begin{aligned} & sU [U^\dagger G_D^{\bar{\chi}}(\omega + \nu)U]_{m_2 s_2, m_s} [U^\dagger G_D^{\bar{\chi}}(\omega)U]_{m_s, m_1 s_1} [U^\dagger G_D^{\bar{\chi}}(\omega' - \nu)U]_{m'_2 s'_2, m'_s} [U^\dagger G_D^{\bar{\chi}}(\omega')U]_{m'_s, m'_1 s'_1} \\ & = sU G_D^{\bar{\chi}, m_2 s_2, m_s}(\omega + \nu) G_D^{\bar{\chi}, m_s, m_1 s_1}(\omega) G_D^{\bar{\chi}, m'_2 s'_2, m'_s}(\omega' - \nu) G_D^{\bar{\chi}, m'_s, m'_1 s'_1}(\omega') e^{i[\phi_{m_2}(\omega + \nu) + \phi_{m'_2}(\omega' - \nu) - \phi_{m_1}(\omega) - \phi_{m'_1}(\omega')]} \end{aligned} \quad (87)$$

It is independent of phase ϕ_m defined on the m th Keldysh contour. The phase cancels because of the conservation of energy: $-\phi_m(\omega + \nu) - \phi_m(\omega' - \nu) + \phi_m(\omega) + \phi_m(\omega') = 0$. Therefore, any closed diagram is independent of the phase ϕ_m since at each bare vertex, the phase cancels [40].

The above discussion implies that at the steady state, operators $\hat{\rho}_A$ and \hat{H}_A are effectively commutative even in the presence of the intra-Coulomb interaction. This is because the energy associated with the coupling between the two subsystems \hat{V} is negligible compared to the net energy transferred to subsystem A , which grows linearly in τ . Because $\hat{\rho}_A$ and \hat{N}_A are commutative [34], we expect

$$[\hat{\rho}_A(\tau), \hat{Q}_A] \approx 0 \quad (88)$$

in the steady state. In other words, in the steady state, the *local* heat quantity is a classical quantity, as anticipated.

VIII. PREVIOUS APPROACH

We compare our approach and the previous quantum information theory approach [9,10]. The previous approach is as follows. The communication channel is characterized by an input (output) alphabet B (A) with letters labeled b (a). The input letter b is encoded in a quantum state $\hat{\rho}_b$. The probability of transmitting the input letter b is $p_B(b)$. The conditional probability of output letter a given input letter b is $p_{A|B}(a|b) = \text{Tr} \hat{\rho}_b \hat{F}_a$, where \hat{F}_a is the effect satisfying $\sum_a \hat{F}_a = \hat{1}$. The capacity is the average mutual information $H(A; B)$ maximized over all possible input distributions $p_B(b)$:

$$C = \frac{1}{\tau} \max_{\{p_B(b)\}} H(A; B),$$

$$H(A; B) = \sum_b p_B(b) \sum_a p_{A|B}(a|b) \ln \frac{p_{A|B}(a|b)}{p_A(a)}, \quad (89a)$$

where $p_A(a) = \sum_b p_{A|B}(a|b) p_B(b)$ is the probability to obtain the output a . A further maximization over measurement schemes and over input states yields the optimum capacity $C_{\text{opt}} = \max_{\{\hat{\rho}_b\}} \max_{\{\hat{F}_a\}} C$. By exploiting Holevo's theorem, $\max_{\{\hat{F}_a\}} H(A; B) \leq S(\hat{\rho}) - \sum_b p_B(b) S(\hat{\rho}_b)$, where $\hat{\rho} = \sum_b p_B(b) \hat{\rho}_b$, one can find a link between the mutual information and the von Neumann entropy: $\max_{\{\hat{\rho}_b\}} \max_{\{\hat{F}_a\}} \max_{\{p_B(b)\}} H(A; B) \leq \max_{\hat{\rho}} S(\hat{\rho})$. The maximum turned out to be the optimum capacity

$$\tau C_{\text{opt}} = \max_{\hat{\rho}} S(\hat{\rho}) = \ln \text{rank} \hat{\rho}. \quad (89b)$$

The rank of the density matrix $\hat{\rho}$ is estimated by counting the number of possible particle-number eigenstates [9,10]. In the following, we assume only electrons above the Fermi

energy carry the information. For a linear dispersion channel, allowed energies are $\Delta E j$, where $j \in \mathcal{S} = \{1, 2, \dots\}$ and $\Delta E = h/\tau$ is the minimum level spacing. Then, the rank of $\hat{\rho}$ is the number of Fock states,

$$|n_1, n_2, \dots\rangle = |\{n_j\}\rangle, \quad (90a)$$

where $n_j = 0, 1$ is the electron occupation number of the mode j . The signal energy corresponds to the energy of the Fock state $|\{n_j\}\rangle$ as

$$P\tau = \sum_{j=1}^{\infty} \Delta E j n_j. \quad (90b)$$

Therefore, when $P\tau/\Delta E = \sum_{j=1}^{\infty} j n_j$ is a positive integer, the number of Fock states with a given energy $P\tau$ is the number of integer partitions into distinct elements of the set \mathcal{S} , $p(P\tau/\Delta E | \text{distinct parts in } \mathcal{S})$. The partition function is, for example, $p(6 | \text{distinct parts in } \mathcal{S}) = 4$ since 6 can be partitioned into 4 ways $6 = 1 + 5 = 2 + 4 = 1 + 2 + 3$. In the end, we obtain

$$\tau C_{\text{opt}} = \ln p(P\tau/\Delta E | \text{distinct parts in } \mathcal{S}), \quad (90c)$$

which is the result obtained previously for fermions in Ref. [10]. The above-mentioned derivation was first applied to bosons in Ref. [9].

One may think that Eq. (89b) is equivalent to Eq. (23), if one regards $\hat{\rho}$ here as $\hat{\rho}_{A, Q_A}$. Precisely speaking, we consider that Eqs. (23) and (89b) would be different. In Ref. [10], it was pointed out that the operators \hat{F}_a and $\hat{\rho}_b$ act on the Fock subspace of left-moving states (in our setup, the information flows from right to left; see Fig. 1). Thus, the right-hand side of Eq. (89b) is the logarithm of the size of the Fock subspace of left movers containing a given total energy. In our approach, the operator $\hat{\rho}_{A, Q_A}$ acts *locally* on the subsystem A , the receiver side. Therefore, our approach accounts for the spatial separation between the transmitter side and the receiver side to a certain extent. On the other hand, we did not calculate the mutual information. Indeed, we do not know how to calculate it based on the Keldysh technique. This problem is beyond the scope of this paper.

IX. SUMMARY

In summary, we have investigated fluctuations of self-information and heat quantity. We bipartition the quantum conductor and regard subsystem A (B) as the receiver (transmitter) side and considered the reduced-density matrix of subsystem A . By exploiting the multicontour Keldysh Green function technique, we calculate the Rényi entropy of a positive integer order subjected to the constraint of the local heat

quantity of subsystem A . By performing the analytic continuation, we relate it to the information-generating function. When the thermal noise of the receiver side is absent, there exists the Jarzynski equalitylike universal relation (5), which relates the Rényi entropy of order 0 at the steady state with the optimum capacity of information transmission. For electrons, the optimum capacity is related to the number of integer partitions into distinct parts. The optimum capacity obtained in this way is consistent with that of the quantum information theory approach [9,10].

We applied our theory to the resonant-level model. The expressions of average self-information and average heat quantity are consistent with those of the previous scattering theory [12,14]. We analyzed the fluctuations of self-information and conditional self-information for a narrow-band channel, for a wide-band channel, and for a resonant tunneling condition. We calculated the correction to the Rényi entropy induced by the onsite Coulomb interaction within the Hartree approximation and checked that the weak Coulomb interaction does not alter the optimum capacity.

We also pointed out that in the steady state, even in the presence of the intra-Coulomb interaction, the reduced-density matrix of subsystem A may be diagonal in the eigenstates of the operator of “local heat quantity” acting locally on subsystem A .

ACKNOWLEDGMENTS

We thank H. Okada and Y. Tokura for the valuable discussions. This work was supported by JSPS KAKENHI Grants No. 17K05575 and No. JP26220711.

APPENDIX A: PROJECTION OPERATOR

Here, we relate Eq. (11) with the standard form of the projection operator [42]. Let $|S_A, j\rangle$ be an orthonormal basis such that

$$\hat{S}_A |S_A, j\rangle = S_A |S_A, j\rangle, \quad j \in \{1, \dots, N_{S_A}\}. \quad (\text{A1})$$

Here, the index j is used to label possible degeneracies. We assumed that the dimensionless heat quantity is discrete, $S_A = \Delta n$, where n is an integer. Then, we obtain

$$\begin{aligned} \langle S_A', j' | \hat{\Pi}_{S_A} |S_A'', j''\rangle &= \frac{\Delta}{2\pi} \int_{-\pi/\Delta}^{\pi/\Delta} d\chi e^{-i\chi(S_A - S_A')} \delta_{S_A', S_A''} \delta_{j', j''} \\ &= \delta_{S_A, S_A'} \delta_{S_A', S_A''} \delta_{j', j''}. \end{aligned} \quad (\text{A2})$$

By combining it with the completeness relation

$$\sum_{S_A} \sum_{j=1}^{N_{S_A}} |S_A, j\rangle \langle S_A, j| = \hat{1}, \quad (\text{A3})$$

the projection operator is rewritten as

$$\hat{\Pi}_{S_A} = \sum_{j=1}^{N_{S_A}} |S_A, j\rangle \langle S_A, j|, \quad (\text{A4})$$

which is the standard form of the rank- N_{S_A} projector (see Chap. 1.2.2 of Ref. [42]). From Eq. (A4), one can derive

$$\hat{\Pi}_{S_A} \hat{\Pi}_{S_A'} = \delta_{S_A, S_A'} \hat{\Pi}_{S_A}. \quad (\text{A5})$$

APPENDIX B: DERIVATION OF EQ. (36)

Here, we write the initial density matrix as $\hat{\rho}_{\text{eq}} = \hat{\rho}_{A\text{eq}} \hat{\rho}_{B\text{eq}}$. Our setup satisfies the following conditions: (i) The *total* particle number is conserved during the time evolution

$$[\hat{H}, \hat{N}_A + \hat{N}_B] = 0. \quad (\text{B1})$$

(ii) The initial state is diagonal in the particle-number sector

$$[\hat{\rho}_{\text{eq}}, \hat{N}_A + \hat{N}_B] = 0, \quad (\text{B2})$$

and in the energy sector of the unperturbed Hamiltonian

$$[\hat{\rho}_{\text{eq}}, \hat{H}_A + \hat{H}_B] = 0. \quad (\text{B3})$$

Then, the commutation relation, the left-hand side of Eq. (36), is

$$[\hat{\rho}_A(\tau), \hat{Q}_A] = [\hat{\rho}_A(\tau), \hat{H}_A] - \mu_A [\hat{\rho}_A(\tau), \hat{N}_A]. \quad (\text{B4})$$

The second term on the right-hand side of Eq. (B4) is further calculated as

$$\begin{aligned} [\hat{\rho}_A(\tau), \hat{N}_A] &= \text{Tr}_B([e^{-i\hat{H}\tau} \hat{\rho}_{\text{eq}} e^{i\hat{H}\tau}, \hat{N}_A + \hat{N}_B]) \\ &\quad - \text{Tr}_B([e^{-i\hat{H}\tau} \hat{\rho}_{\text{eq}} e^{i\hat{H}\tau}, \hat{N}_B]). \end{aligned} \quad (\text{B5})$$

The first line of the right-hand side is zero because of Eqs. (B1) and (B2). The second line of the right-hand side is also zero from the cyclic property of the partial trace over the subsystem B :

$$\text{Tr}_B([\hat{O}, \hat{N}_B]) = 0. \quad (\text{B6})$$

Here, an operator \hat{O} acts on the subsystems A and B . Therefore, Eq. (B5) is zero, which is the consequence of the local-particle-number superselection (see Appendix A of Ref. [34]).

By exploiting Eqs. (B3) and (B6), the first term on the right-hand side of Eq. (B4) is transformed as

$$\begin{aligned} [\hat{\rho}_A(\tau), \hat{H}_A] &= \text{Tr}_B([e^{-i\hat{H}\tau} \hat{\rho}_{\text{eq}} e^{i\hat{H}\tau}, \hat{H}]) \\ &\quad - \text{Tr}_B([e^{-i\hat{H}\tau} \hat{\rho}_{\text{eq}} e^{i\hat{H}\tau}, \hat{H}_B + \hat{V}]) \end{aligned} \quad (\text{B7})$$

$$\begin{aligned} &= \text{Tr}_B(e^{-i\hat{H}\tau} [\hat{\rho}_{\text{eq}}, \hat{V}] e^{i\hat{H}\tau}) \\ &\quad - \text{Tr}_B([e^{-i\hat{H}\tau} \hat{\rho}_{\text{eq}} e^{i\hat{H}\tau}, \hat{V}]) \end{aligned} \quad (\text{B8})$$

$$= \text{Tr}_B(e^{-i\hat{H}\tau} [\hat{\rho}_{\text{eq}}, \hat{V} - e^{i\hat{H}\tau} \hat{V} e^{-i\hat{H}\tau}] e^{i\hat{H}\tau}). \quad (\text{B9})$$

In general, Eq. (B9) is not necessarily zero. By summarizing above, we obtain Eq. (36).

APPENDIX C: EXPLICIT EXPRESSIONS OF THE MULTICONTOUR KELDYSH GREEN FUNCTION

A $2M \times 2M$ Keldysh Green function matrix \mathbf{g}_A consists of 2×2 submatrices in the normal Keldysh space.

A (m, m') component ($m, m' = 1, \dots, M$) is

$$\begin{aligned} [\mathbf{g}_A^{\{\chi_j\}}(t, t')]_{m, m'} &= \begin{bmatrix} g_A^{\{\chi_j\}, m+, m'+} & g_A^{\{\chi_j\}, m+, m'-} \\ g_A^{\{\chi_j\}, m-, m'+} & g_A^{\{\chi_j\}, m-, m'-} \end{bmatrix} \\ &= -ie^{-i\epsilon_A(t-t')} \begin{cases} e^{i\sum_{j=m'}^{m-1} \delta\chi_j s_A} \begin{bmatrix} f_{A, m-m'}^{\bar{\chi}}(\epsilon_A) & f_{A, m-m'+1}^{\bar{\chi}}(\epsilon_A) e^{-i\bar{\chi}s_A/M} \\ f_{A, m-m'-1}^{\bar{\chi}}(\epsilon_A) e^{i\bar{\chi}s_A/M} & f_{A, m-m'}^{\bar{\chi}}(\epsilon_A) \end{bmatrix} & (m > m') \\ \begin{bmatrix} f_{A, 0}^{\bar{\chi}}(\epsilon_A)\theta(t-t') - f_{A, M}^{\bar{\chi}}(\epsilon_A)\theta(t'-t) & f_{A, 1}^{\bar{\chi}}(\epsilon_A) e^{-i\bar{\chi}s_A/M} \\ -f_{A, M-1}^{\bar{\chi}}(\epsilon_A) e^{i\bar{\chi}s_A/M} & f_{A, 0}^{\bar{\chi}}(\epsilon_A)\theta(t'-t) - f_{A, M}^{\bar{\chi}}(\epsilon_A)\theta(t-t') \end{bmatrix} & (m = m') \\ e^{-i\sum_{j=m}^{m'-1} \delta\chi_j s_A} \begin{bmatrix} -f_{A, M+m-m'}^{\bar{\chi}}(\epsilon_A) & -f_{A, M+m-m'+1}^{\bar{\chi}}(\epsilon_A) e^{-i\bar{\chi}s_A/M} \\ -f_{A, M+m-m'-1}^{\bar{\chi}}(\epsilon_A) e^{i\bar{\chi}s_A/M} & -f_{A, M+m-m'}^{\bar{\chi}}(\epsilon_A) \end{bmatrix} & (m < m'), \end{cases} \end{aligned} \quad (\text{C1})$$

where we write $s_A = s_A(\epsilon_A)$. The modified Fermi distribution function is given by

$$f_{A, m}^{\bar{\chi}}(\omega) = \frac{e^{-m(1-i\bar{\chi}/M)s_A(\omega)}}{1 + e^{-M(1-i\bar{\chi}/M)s_A(\omega)}}. \quad (\text{C2})$$

Equation (C1) is Eq. (57) in Ref. [34] replaced χ_j with $\chi_j s_A$. For detailed derivations, see Ref. [34].

The $2M \times 2M$ Keldysh Green function matrix $\mathbf{g}_A^{\bar{\chi}}$ in Eq. (39b) is obtained after the Fourier transform in time. It is a block skew-circulant

$$\mathbf{g}_A^{\bar{\chi}}(\omega) = \begin{bmatrix} \mathbf{A}_0 & -\mathbf{A}_{M-1} & -\mathbf{A}_{M-2} & \cdots & -\mathbf{A}_1 \\ \mathbf{A}_1 & \mathbf{A}_0 & -\mathbf{A}_{M-1} & \cdots & -\mathbf{A}_2 \\ \mathbf{A}_2 & \mathbf{A}_1 & \mathbf{A}_0 & \cdots & -\mathbf{A}_3 \\ \vdots & \vdots & \vdots & \ddots & \vdots \\ \mathbf{A}_{M-1} & \mathbf{A}_{M-2} & \mathbf{A}_{M-3} & \cdots & \mathbf{A}_0 \end{bmatrix}. \quad (\text{C3})$$

A diagonal component is

$$\begin{aligned} \mathbf{A}_0 &= \text{P} \frac{1}{\omega - \epsilon_A} \boldsymbol{\tau}_3 - 2\pi i \delta(\omega - \epsilon_A) \\ &\times \begin{bmatrix} 1/2 - f_{A, M}^{\bar{\chi}}(\omega) & f_{A, 1}^{\bar{\chi}}(\omega) e^{-i\frac{\bar{\chi}}{M}s_A(\omega)} \\ -f_{A, M-1}^{\bar{\chi}}(\omega) e^{i\frac{\bar{\chi}}{M}s_A(\omega)} & 1/2 - f_{A, M}^{\bar{\chi}}(\omega) \end{bmatrix}, \end{aligned} \quad (\text{C4})$$

where $\boldsymbol{\tau}_3 = \text{diag}(1, -1)$. The phase factor $e^{-i\bar{\chi}s_A(\omega)/M}$ is equivalent to what appears in the full counting statistics [43–46] of heat current [47–53]. The delta function is

$$\delta(\omega) = \text{Im} \frac{1}{\pi(\omega - i\eta)}, \quad (\text{C5a})$$

where η is a positive infinitesimal. P stands for the Cauchy principal value

$$\text{P} \frac{1}{\omega} = \text{Re} \frac{1}{\omega - i\eta}. \quad (\text{C5b})$$

An off-diagonal component is

$$\begin{aligned} \mathbf{A}_m &= -2\pi i \delta(\omega - \epsilon_A) \\ &\times \begin{bmatrix} f_{A, m}^{\bar{\chi}}(\omega) & f_{A, m+1}^{\bar{\chi}}(\omega) e^{-i\frac{\bar{\chi}}{M}s_A(\omega)} \\ f_{A, m-1}^{\bar{\chi}}(\omega) e^{i\frac{\bar{\chi}}{M}s_A(\omega)} & f_{A, m}^{\bar{\chi}}(\omega) \end{bmatrix}, \end{aligned} \quad (\text{C6})$$

where $m = 1, \dots, M-1$.

The block-skew circulant matrix is block diagonalized by the following discrete Fourier transform [33,34]:

$$\mathbf{g}_A^{\lambda_\ell - \bar{\chi}s_A(\omega)/M} = \sum_{m=m'=0}^{M-1} [\mathbf{g}_A^{\bar{\chi}}]_{m, m'} e^{i\pi \frac{2\ell+1}{M}(m-m')}, \quad (\text{C7})$$

where $\lambda_\ell = \pi[1 - (2\ell + 1)/M]$ and the 2×2 Green function matrix in the left-hand side is

$$\begin{aligned} \mathbf{g}_A^\lambda(\omega) &= \text{P} \frac{1}{\omega - \epsilon_A} \boldsymbol{\tau}_3 - 2\pi i \delta(\omega - \epsilon_A) \\ &\times \begin{bmatrix} 1/2 - f_{A, \lambda}^+(\omega) & f_{A, \lambda}^+(\omega) e^{i\lambda} \\ -f_{A, \lambda}^-(\omega) e^{-i\lambda} & 1/2 - f_{A, \lambda}^+(\omega) \end{bmatrix}. \end{aligned} \quad (\text{C8})$$

Equation (C8) is the modified Keldysh Green function appeared in the theory of the full counting statistics [40,45,46,54–62]. Precisely, the standard scheme of the full counting statistics is based on the two-time measurement protocol, which means that the measurement is done twice: once in the beginning and once in the end [40,46]. In the present case, the measurement is effectively done once in the end [35]. Because of this difference, the electron and hole distribution functions are modified:

$$f_{A, \lambda}^+(\omega) = \frac{f_A^+(\omega)}{f_A^+(\omega) + f_A^-(\omega) e^{i\lambda}}, \quad f_{A, \lambda}^-(\omega) = 1 - f_{A, \lambda}^+(\omega). \quad (\text{C9})$$

The Fourier transform of the $2M \times 2M$ Keldysh Green function matrix for subsystem B [see Eq. (40)] is

$$\mathbf{g}_B(\omega) = \mathbf{1} \otimes \mathbf{g}_B(\omega), \quad (\text{C10})$$

$$\begin{aligned} \mathbf{g}_B(\omega) &= \text{P} \frac{1}{\omega - \epsilon_B} \boldsymbol{\tau}_3 - 2\pi i \delta(\omega - \epsilon_B) \\ &\times \begin{bmatrix} 1/2 - f_B^+(\omega) & f_B^+(\omega) \\ -f_B^-(\omega) & 1/2 - f_B^+(\omega) \end{bmatrix}, \end{aligned} \quad (\text{C11})$$

where $\mathbf{1}$ is the $M \times M$ identity matrix.

APPENDIX D: DOT GREEN FUNCTION MATRIX

The self-energy of the Dyson equation (47) is $\sum_k (J_L^2 \mathbf{g}_{Lk}^\lambda + J_R^2 \mathbf{g}_{Rk}) = \Sigma_L^\lambda + \Sigma_R^{\lambda=0}$, where

$$\Sigma_r^\lambda(\omega) = -i \frac{\Gamma_r}{2} \begin{bmatrix} 1 - 2f_{r,\lambda}^+(\omega) & 2f_{r,\lambda}^+(\omega)e^{i\lambda} \\ -2f_{r,\lambda}^-(\omega)e^{-i\lambda} & 1 - 2f_{r,\lambda}^+(\omega) \end{bmatrix}. \quad (\text{D1})$$

By paying attention to Eqs. (C5a) and (C5b), the matrix inverse of the bare dot Green function matrix, i.e., Eq. (C11) replaced B with D , is calculated as

$$\mathbf{g}_D(\omega)^{-1} = (\omega - \epsilon_D) \boldsymbol{\tau}_3 + 2i\eta \boldsymbol{\tau}_3 \begin{bmatrix} 1/2 - f_D^+(\omega) & f_D^+(\omega) \\ -f_D^-(\omega) & 1/2 - f_D^+(\omega) \end{bmatrix} \boldsymbol{\tau}_3. \quad (\text{D2})$$

The second term of the right-hand side depends on the parameters β_D and μ_D characterizing the initial dot state, through the electron distribution function $f_D^+(\omega) = 1/(e^{-\beta_D(\omega - \mu_D)} + 1)$. It is noticed that these parameters disappear in the steady state, as we anticipated, because the second term of Eq. (D2) is proportional to the positive infinitesimal η and thus is negligible as compared with the self-energy in the Dyson Eq. (47). Then, the solution is independent of these parameters as

$$\mathcal{G}_D^\lambda(\omega) = \frac{\mathcal{G}_D(\omega)}{\Omega_{1,\lambda}(\omega)} + \rho(\omega) \frac{\Gamma_L}{\Gamma} \frac{2\pi i(1 - e^{i\lambda})}{\tilde{f}_L^+(\omega) + \tilde{f}_L^-(\omega)e^{i\lambda}} \begin{bmatrix} f_L^+(\omega)f_L^-(\omega) & f_L^+(\omega)^2 \\ f_L^-(\omega)^2 & f_L^+(\omega)f_L^-(\omega) \end{bmatrix}, \quad (\text{D3})$$

where the DOS of dot is $\rho(\omega) = \mathcal{T}(\omega)\Gamma/(2\pi\Gamma_L\Gamma_R)$ and

$$\mathcal{G}_D(\omega) = \frac{2\pi}{\Gamma} \rho(\omega) \begin{bmatrix} \omega - \epsilon_D - i \sum_r \Gamma_r [1/2 - f_r^+(\omega)] & -i \sum_r \Gamma_r f_r^+(\omega) \\ i \sum_r \Gamma_r f_r^-(\omega) & \epsilon_D - \omega - i \sum_r \Gamma_r [1/2 - f_r^+(\omega)] \end{bmatrix}. \quad (\text{D4})$$

The following relations can be derived by exploiting Eq. (E1):

$$\sum_{\ell=0}^{M-1} \frac{1}{\Omega_{1,\lambda_\ell - \chi_{SA}(\omega)/M}(\omega)} = M - \frac{\partial_{\epsilon_D} \ln \Omega_{M, -\chi_{SA}(\omega)/M}(\omega)}{\partial_{\epsilon_D} \ln \rho(\omega)}, \quad (\text{D5})$$

$$\sum_{\ell=0}^{M-1} \frac{1 - e^{i\lambda_\ell - i\chi_{SA}(\omega)/M}}{\tilde{f}_L^+(\omega) + \tilde{f}_L^-(\omega)e^{i\lambda_\ell - i\chi_{SA}(\omega)/M}} = \frac{\partial_{\epsilon_D} \ln \Omega_{M, -\chi_{SA}(\omega)/M}(\omega)}{\partial_{\epsilon_D} \ln \rho(\omega) \mathcal{T}(\omega) [f_R^+(\omega) - f_L^+(\omega)]}. \quad (\text{D6})$$

Then, the local Green function in the replicated Keldysh space is

$$[\mathcal{G}_D^\lambda(\omega)]_{m,m} = \frac{1}{M} \sum_{\ell=0}^{M-1} \mathcal{G}_D^{\lambda_\ell - \chi_{SA}(\omega)/M}(\omega) = \mathcal{G}_D(\omega) \quad (\text{D7})$$

$$- \frac{1}{M} \frac{\partial_{\epsilon_D} \ln \Omega_{M, -\chi_{SA}(\omega)/M}(\omega)}{\partial_{\epsilon_D} \ln \rho(\omega)} \left(\mathcal{G}_D(\omega) - \frac{2\pi i (\Gamma_L/\Gamma) \rho(\omega)}{\mathcal{T}(\omega) [f_R^+(\omega) - f_L^+(\omega)]} \begin{bmatrix} f_L^+(\omega)f_L^-(\omega) & f_L^+(\omega)^2 \\ f_L^-(\omega)^2 & f_L^+(\omega)f_L^-(\omega) \end{bmatrix} \right). \quad (\text{D8})$$

The result does not change when we account for the spin degree of freedom.

APPENDIX E: SUMMATION

The summation over ℓ in Eq. (46) can be done by exploiting the following relation [63]. Let g be a function. The summation is rewritten as the contour integral as

$$\begin{aligned} \sum_{\ell=0}^{M-1} g(e^{i\lambda_\ell}) &= \int_{C_{\text{odd}}} \frac{du}{2\pi i} \sum_{\ell=0}^{M-1} \frac{g(u)}{u - e^{i\lambda_\ell}} \\ &= \int_{C_{\text{odd}}} \frac{du}{2\pi i} \frac{-M(-u)^{M-1}}{1 + (-u)^M} g(u), \quad (\text{E1}) \end{aligned}$$

where $\lambda_\ell = \pi[1 - (2\ell + 1)/M]$. The contour C_{odd} encloses M poles $e^{i\lambda_\ell}$ ($\ell = 0, \dots, M-1$) (see Fig. 9).

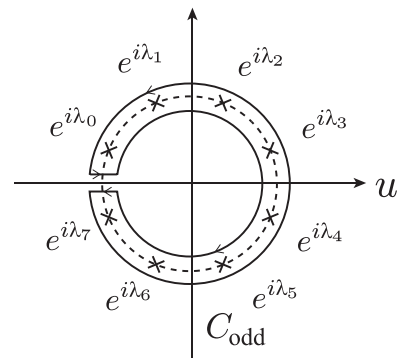


FIG. 9. Contour C_{odd} enclosing poles $e^{i\lambda_\ell}$ ($\ell = 0, \dots, M-1$) ($M = 8$ in this panel). The dotted line indicates a unit circle.

- [1] H. J. Bremermann, in *Proceedings of the Fifth Berkeley Symposium on Mathematical Statistics and Probability*, edited by L. M. LeCam and J. Neyman (University of California Press, Berkeley, 1967); *Int. J. Theor. Phys.* **21**, 203 (1982).
- [2] R. Landauer and J. W. F. Woo, in *Synergetics*, edited by H. Haken (B. G. Teubner, Stuttgart, 1973).
- [3] R. Landauer, *Science* **272**, 1914 (1996).
- [4] S. Lloyd, *Nature (London)* **406**, 1047 (2000).
- [5] D. S. Lebedev and L. B. Levitin, *Dokl. Akad. Nauk SSSR* **149**, 1299 (1963) [*Sov. Phys.–Dokl.* **8**, 377 (1963)]; D. S. Lebedev and L. B. Levitin, *Inf. Control* **9**, 1 (1966).
- [6] J. P. Gordon, in *Quantum Electronics and Coherent Light, Proceedings of the International School of Physics Enrico Fermi, Course XXXI*, edited by P. A. Miles (Academic Press, New York, 1964), p. 156.
- [7] H. Takahashi, in *Advances in Communications Systems*, edited by A. V. Balakrishnan (Academic Press, New York, 1965), Vol. 1, p. 227.
- [8] J. B. Pendry, *J. Math. A: Math. Gen.* **16**, 2161 (1983).
- [9] C. M. Caves and P. D. Drummond, *Rev. Mod. Phys.* **66**, 481 (1994).
- [10] M. P. Blencowe and V. Vitelli, *Phys. Rev. A* **62**, 052104 (2000).
- [11] C. E. Shannon, *Bell System Technol. J.* **27**, 379 (1948).
- [12] U. Sivan and Y. Imry, *Phys. Rev. B* **33**, 551 (1986).
- [13] G. E. Andrews and K. Eriksson, *Integer Partitions* (Cambridge University Press, Cambridge, 2004).
- [14] E. Akkermans, *Eur. Phys. J. E* **28**, 199 (2009).
- [15] T. M. Cover and J. A. Thomas, *Elements of Information Theory*, 2nd ed. (Wiley-Interscience, New York, 2006).
- [16] H. Li and F. D. M. Haldane, *Phys. Rev. Lett.* **101**, 010504 (2008).
- [17] H. F. Song, S. Rachel, C. Flindt, I. Klich, N. Laflorencie, and K. Le Hur, *Phys. Rev. B* **85**, 035409 (2012).
- [18] A. Petrescu, H. F. Song, S. Rachel, Z. Ristivojevic, C. Flindt, N. Laflorencie, I. Klich, N. Regnault, and K. Le Hur, *J. Stat. Mech.* (2014) P10005.
- [19] R. M. Fano, *Transmission of Information: A Statistical Theory of Communications* (MIT Press, Cambridge, MA, 1961).
- [20] S. W. Golomb, *IEEE Trans. Inf. Theory* **IT-12**, 75 (1966).
- [21] S. Guiasu and C. Reischer, *Inf. Sci.* **35**, 235 (1985).
- [22] A. Rényi, in *Proceedings of the Fourth Berkeley Symposium on Mathematics, Statistics, and Probability* (University of California Press, Berkeley, CA, 1960), p. 547.
- [23] Precisely, the Rényi entropy of probability distribution $P = (p_1, \dots, p_n)$ is [22] $\log(\sum_{k=1}^n p_k^\alpha)/(\alpha - 1)$ where $\alpha \neq 1$. In this paper, we call $\sum_{k=1}^n p_k^\alpha$ as the Rényi entropy.
- [24] M. Campisi, P. Hänggi, and P. Talkner, *Rev. Mod. Phys.* **83**, 771 (2011).
- [25] C. Jarzynski, *Phys. Rev. Lett.* **78**, 2690 (1997).
- [26] M. F. Ludovico, J. S. Lim, M. Moskalets, L. Arrachea, and D. Sánchez, *Phys. Rev. B* **89**, 161306(R) (2014).
- [27] M. Esposito, M. A. Ochoa, and M. Galperin, *Phys. Rev. Lett.* **114**, 080602 (2015).
- [28] M. Esposito, M. A. Ochoa, and M. Galperin, *Phys. Rev. B* **92**, 235440 (2015).
- [29] M. A. Ochoa, A. Bruch, and A. Nitzan, *Phys. Rev. B* **94**, 035420 (2016).
- [30] M. F. Ludovico, M. Moskalets, D. Sánchez, and L. Arrachea, *Phys. Rev. B* **94**, 035436 (2016).
- [31] Yu. V. Nazarov, *Phys. Rev. B* **84**, 205437 (2011).
- [32] M. H. Ansari and Yu. V. Nazarov, *Phys. Rev. B* **91**, 104303 (2015); *Zh. Eksp. Teor. Fiz.* **149**, 453 (2016) [*J. Exp. Theor. Phys.* **122**, 389 (2016)]; M. H. Ansari, *Phys. Rev. B* **95**, 174302 (2017).
- [33] Y. Utsumi, *Phys. Rev. B* **92**, 165312 (2015).
- [34] Y. Utsumi, *Phys. Rev. B* **96**, 085304 (2017).
- [35] Y. Utsumi, *Eur. Phys. J. Spec. Top.* (2019), doi:10.1140/epjst/e2018-800043-4.
- [36] M. H. Ansari and Yu. V. Nazarov, *Phys. Rev. B* **91**, 174307 (2015).
- [37] H. Touchette, *Phys. Rep.* **478**, 1 (2009).
- [38] M. A. Nielsen and I. L. Chuang, *Quantum Computation and Quantum Information* (Cambridge University Press, New York, 2000).
- [39] N. W. Ashcroft, N. D. Mermin, and D. Wei, *Solid State Physics: Revised Edition* (Centage Learning Asia, Singapore, 2016).
- [40] K. Saito and Y. Utsumi, *Phys. Rev. B* **78**, 115429 (2008).
- [41] L. G. C. Rego and G. Kirczenow, *Phys. Rev. Lett.* **81**, 232 (1998).
- [42] H. M. Wiseman and G. J. Milburn, *Quantum Measurement and Control* (Cambridge University Press, Cambridge, 2010).
- [43] L. S. Levitov, H. W. Lee, and G. B. Lesovik, *J. Math. Phys.* **37**, 4845 (1996).
- [44] *Quantum Noise in Mesoscopic Physics, Vol. 97 of NATO Science Series II: Mathematics, Physics and Chemistry*, edited by Yu. V. Nazarov (Kluwer, Dordrecht, 2003).
- [45] D. A. Bagrets, Y. Utsumi, D. S. Golubev, and G. Schön, *Fortschr. Phys.* **54**, 917 (2006).
- [46] M. Esposito, U. Harbola, and S. Mukamel, *Rev. Mod. Phys.* **81**, 1665 (2009).
- [47] M. Kindermann and S. Pilgram, *Phys. Rev. B* **69**, 155334 (2004).
- [48] K. Saito and A. Dhar, *Phys. Rev. Lett.* **99**, 180601 (2007).
- [49] T. T. Heikkilä and Yu. V. Nazarov, *Phys. Rev. Lett.* **102**, 130605 (2009).
- [50] M. A. Laakso, T. T. Heikkilä, and Yu. V. Nazarov, *Phys. Rev. Lett.* **104**, 196805 (2010); *Phys. Rev. B* **82**, 205316 (2010); **85**, 184521 (2012).
- [51] D. Golubev, T. Faivre, and J. P. Pekola, *Phys. Rev. B* **87**, 094522 (2013).
- [52] Y. Utsumi, O. Entin-Wohlman, A. Aharony, T. Kubo, and Y. Tokura, *Phys. Rev. B* **89**, 205314 (2014).
- [53] P. Wollfarth, A. Shnirman, and Y. Utsumi, *Phys. Rev. B* **90**, 165411 (2014); P. Wollfarth, Y. Utsumi, and A. Shnirman, *ibid.* **96**, 064302 (2017).
- [54] Y. Utsumi, D. S. Golubev, and Gerd Schön, *Phys. Rev. Lett.* **96**, 086803 (2006).
- [55] A. O. Gogolin and A. Komnik, *Phys. Rev. B* **73**, 195301 (2006).
- [56] Y. Utsumi and K. Saito, *Phys. Rev. B* **79**, 235311 (2009).
- [57] D. F. Urban, R. Avriiler, and A. Levy Yeyati, *Phys. Rev. B* **82**, 121414(R) (2010).
- [58] R. Sakano, A. Oguri, T. Kato, and S. Tarucha, *Phys. Rev. B* **83**, 241301(R) (2011); R. Sakano, Y. Nishikawa, A. Oguri, A. C. Hewson, and S. Tarucha, *Phys. Rev. Lett.* **108**, 266401 (2012).

- [59] T. Novotný, F. Haupt, and W. Belzig, *Phys. Rev. B* **84**, 113107 (2011).
- [60] Y. Utsumi, O. Entin-Wohlman, A. Ueda, and A. Aharony, *Phys. Rev. B* **87**, 115407 (2013).
- [61] G-M. Tang and J. Wang, *Phys. Rev. B* **90**, 195422 (2014).
- [62] R. Seoane Souto, R. Avriller, R. C. Monreal, A. Martín-Rodero, and A. Levy Yeyati, *Phys. Rev. B* **92**, 125435 (2015).
- [63] H. Casini and M. Huerta, *J. Phys. A: Math. Gen.* **42**, 504007 (2009).